ADVANCED RISK STRATIFICATION AND PREDICTION OF VENOUS THROMBOEMBOLISM IN CRITICALLY ILL PATIENTS

by
A. Meiyappan

A thesis submitted to The Johns Hopkins University in conformity
with the requirements for the degree of Masters in Biomedical Engineering

Baltimore, Maryland
MAY, 2021

Abstract

Venous Thromboembolism (VTE) is a disease responsible for more than 100,000 deaths a year in the U.S [1]. Thru early detection, this mortality rate can be decreased as the early administration of therapeutic heparin can prevent VTE from being fatal. However, this can be challenging in a surgical ICU setting where symptoms can hard to distinguish from common ICU patient symptoms [2]. In this work, we developed a risk prediction model and a novel real time classification model to determine the risk of VTE. The risk prediction model analyzes patient demographic and history data to determine if they are at a high risk. Meanwhile, the real time classification model analyzes high frequency physiological time series data to determine if a patient is currently experiencing a VTE. The findings from this study and model will be implemented as a screening tool to assist clinicians in determining which patients require additional care.

Thesis Readers

Dr. Adam Sapirstein (Primary Advisor)
Associate Professor
Anesthesiology and Critical Care Medicine
School of Medicine
Johns Hopkins University

Dr. Joseph L. Greenstein
Associate Research Scientist
Institute for Computational Medicine
Whiting School of Engineering
Johns Hopkins University

Dr. Raimond Winslow
Professor
SOM Biomedical Engineering, Computational Biology and Bioinformatics
School of Medicine
Johns Hopkins University

Dr. Brian S Caffo
Professor
Biostatistics Faculty
School of Public Health
Johns Hopkins University

Dedicated to my wonderful mother and father

for all the love and support they have shown over the years

Thank you Love Akilan.

Acknowledgements

I have so many people to thank and acknowledge. To start with, thank you to my thesis advisor, Dr. Adam Sapirstein, for all the time and effort you have spent working with me on this project. I know you are a busy person, but it meant a lot to me that you would still set aside time to work on this project with me. I hope you enjoyed this experience as much as I did.

I would like to thank Dr.Steve Cho, my first mentor in the Johns Hopkins ecosystem back when I was just a senior in high school. Although I was in high school, this experience was my first biomedical engineering project which started my passion for the field. Also, I must thank Dr. Michael Jacobs, my mentor at Hopkins for the summers of 2015 and 2016. During my time with Dr.Jacobs, I got to work on some cool projects such as mapping Apparent Diffusion factor or Coefficient (ADC) of water molecules in tissues for cancer detection, and analyzing clinical breast cancer reports using Natural Language Processing (NLP). Thank you Dr. Jacobs for allowing me to work on some very fun and interesting projects which undoubtedly grew my passion for biomedical engineering. Next I would like to thank Dr.Ishan Barman, in the mechanical engineering department at Johns Hopkins University. Under Dr.Barman, I would work on my first data science project, image classification of cell images. This project would represent the final straw to push me into studying biomedical engineering with a focus of data science, a sharp distinction from my mechanical engineering undergraduate degree.

I must also thank my family and friends, for the continued support and love they

have shown throughout this whole process. They have helped every step of the way and have always been supporting even when times are difficult. I will be ever grateful for the love and support.

Finally, I would like to thank a couple of individuals from Johns Hopkins University whom have helped me along the way. I would like to thank Dr.Greenstein and Dr.Winslow, for teaching me the process of proper research, and providing critical feedback early on during this project. I would also like to thank Dr.Caffo, for teaching me the necessary skills and techniques in order to be an exceptional data scientist. Lastly, I would like to thank my Team Mola Mola members from my Precision Care Medicine class, Jinrui Lui, Bronte Wen and Elizabeth Wu. Thank you for all the hard work and effort you gave in beginning of this project.

If it was not for all of you, I would not have been able to write this thesis.

Contents

List of Tables

List of Figures

Chapter 1

Introduction

Venous Thromboembolism (VTE) is a common but preventable disease that encompasses two medical complications, Deep Vein Thrombosis (DVT) and Pulmonary Embolism (PE). In a 2008 Report, the Surgeon General of the United States approximated that VTE accounts for more than 100,000 deaths per year in the US [1]. Healthcare associated VTE risk is increased by surgery, trauma, or prolonged bed-rest, thus putting most patients in a surgical ICU at increased risk for VTE [2]. Furthermore, out of all patients who have symptoms of VTE, only 25% of symptomatic patients actually have a thrombus, thus making the disease hard to distinguish from common symptoms patients experience in the ICU [2]. In hospitalized patients, most VTE presents as a Deep Vein Thrombosis, or Pulmonary Embolism. Most of the serious morbidities and mortality are related to PE, which can prevent blood flow to the lungs. The most effective prophylaxis and treatment for VTE is to administer heparin, however this intervention comes with a serious risk of bleeding complications [3]. Additionally, approximately 5% to 10% of patients treated with heparin for thrombosis develop thrombocytopenia, a morbid complication involving low platelet count [4]. Therefore, there has been an emphasis placed on developing and using Risk Assessment Models (RAMs) to ensure that VTE prophylaxis is appropriately provided to hospitalized patients. Currently there is no standard risk assessment model for VTE in a hospitalized [5] or ICU setting. For a majority of ICU patients, the standard

therapy is a combination of pharmacologic and mechanical prophylaxis. In spite of this, almost 10% of surgical ICU patients have a VTE incident [6]. In post-surgical patients, risk assessment and bedside diagnosis is particularly problematic, as this patient population has preexisting risk factors that include tissue injury, stasis and many also have a cancer diagnosis, all of which are known to increase the probability of a VTE. In addition the usefulness of D-dimer, a test measuring fibrin deposition indicative of thrombus formation [7], in risk assessment algorithms is usually minimized by its elevation following surgery. Current machine learning methods are specified for Risk Prediction rather than Real Time Analysis, and provide information for specific scenarios, such as using Risk Assessment Models (RAMs) for VTE in post-chemotherapy cancer patients [8] or predicting VTE complications following Posterior Lumbar Spine Fusion surgery [9]. Outpatient clinical scoring systems such as the Modified Wells' Criteria have poor sensitivity in intensive care settings as several of the risk factors that influence the probability of the disease are already present in a majority of patients. Futhermore, machine learning approaches for VTE risk stratification utilize components of the Wells' score and thus face many of the same difficulties in application to the ICU setting [10]. More complex risk assessment models such as the Caprini model and Padua prediction score have improved performance over these clinical scoring systems but still have significant room for improvement in sensitivity, specificity, and patient outcomes [11–13]. The common factor of the currently available models is their use of static data measurements to approximate risk throughout the patients stay, and thus more effective in an out-patient medical settings and do not apply well to critically ill patient populations, causing clinicians to struggle to accurately detect VTE. Moreover, diagnosis of VTE is typically in the late stages as the onset of the disease is often asymptomatic. The current diagnostic approach is dependent on patient reported symptoms as well as physiologic parameters. Therefore, developing a robust and comprehensive predictive analysis algorithm can

inform doctors in advance whether or not patients are at an increased risk of developing VTE, and start treatment early.

The development of VTE is a dynamic process and coagulability can change on a daily basis. There are vast amounts of real-time data produced by patients in the ICU that currently is unused in the assessment of risk for VTE. The inclusion of these time varying parameters will improve the specificity of previous risk assessment models, and will lead to the development of a real-time risk prediction system for VTE that takes into account the daily fluctuations in the patient's physiologic state. The objectives of this study were to determine if the inclusion of an expanded feature set in non-biased mathematical models could improve on the current performance of existing RAMs when applied in ICU patients and if the addition of physiologic time series (PTS) data can be used for diagnostic screening of VTE in surgical ICU patients.

Chapter 2

Methods

2.1 Data

The data used was collected between 2016 and 2017 using the Anesthesia Quality Improvement data base of the Department of Anesthesiology and Critical Care Medicine at Johns Hopkins School of Medicine. The data set was de-identified before use and contains 10,180 unique patients' data.

2.2 Preprocessing Data and Cohort Definitions

The categorization of VTE encompasses two clinical outcomes, PE and DVT. ICD 10 codes were used to identify positive VTE patients.

The codes, located in Table 2-1, were narrowed down to new, acute VTE, excluding codes for chronic VTE, septic PEs, and codes relating to superficial veins. After filtering by ICD 10 Codes, 265 VTE patients were identified with 135 DVT patients, 87 PE patients and 43 DVT + PE patients. Figure 2-1 depicts the filtration process.

Table 2-1. ICD10 Codes

ICD10 Codes	
DVT Codes	PE Codes
I82.4/x/xx	126
182.60/x	126.0
182.62x	126.02
182.A1/x	126.09
182.B1/x	126.9
I82.C1/x	126.92
	126.99
	O88.2/X/XX

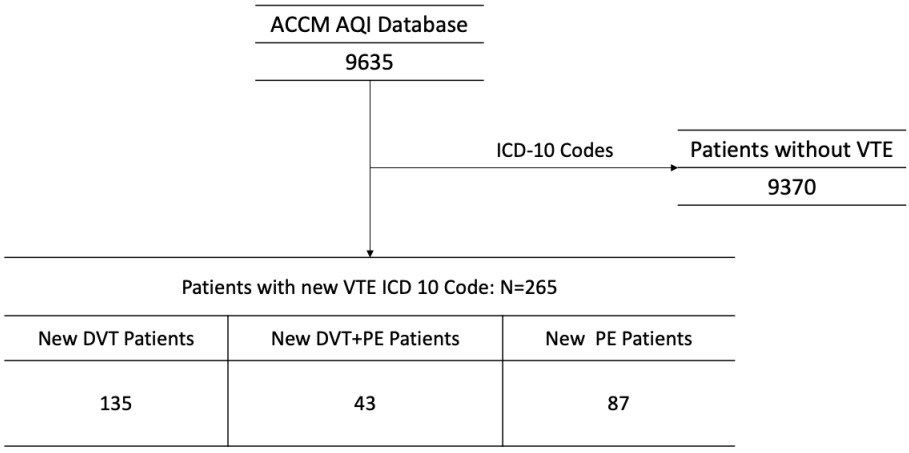

Figure 2-1. Patient Cohort Selection for VTE Risk Prediction

The set of inclusion/exclusion criteria described in Figure 2-1 was used to generate a population for the development of a preliminary risk assessment score. In order to determine proper time windows for the time sensitive VTE classification model, a more rigorous approach was needed. Patients were screened by their ICD-10 codes, then further screened by the presence of an imaging scan and therapeutic heparin administration. Through this filtration process, depicted in Figure 2-2, 51 VTE patients were identified within in the original population, with 26 new DVT, 18 new

PE, and 7 new DVT+PE patients.

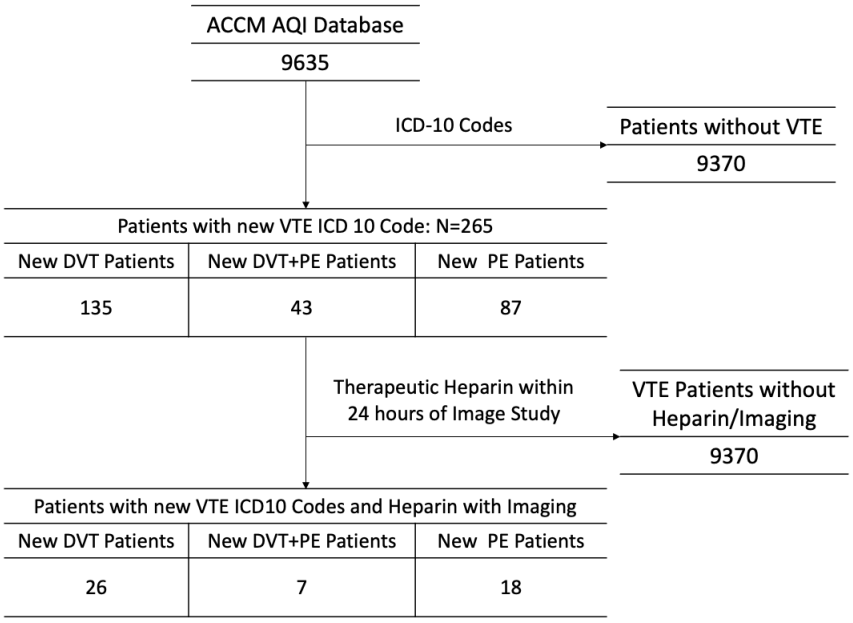

Figure 2-2. Patient Cohort Filtration for Real-Time VTE Classification

For the Risk Prediction Model, the following nine data categories were extracted: age, sex, weight, height, ASA Physical Status, smoking history, race, type of surgery, and the patient's comorbidities at the time of their admission to the hospital. These nine data categories corresponded to 96 features for modeling since patients could have multiple features in some of the categories. For example, comorbidities were administratively assigned to patients using the set of 30 Elixahuser comorbidity measures [14]. The Real-Time VTE Classification included an additional six statistical elements derived from physiologic time-series data. These data elements were: Arterial Mean Blood Pressure, Arterial Systolic Blood Pressure, Arterial Diastolic Blood Pressure, Oxygen Saturation, Heart Rate and Respiratory Rate, which were extracted using the R-package tsfeatures [15].

2.3 VTE Risk Prediction Model

The first goal was to develop a generalized risk assessment model to estimate the probability of a post-surgical ICU patient developing a VTE during their hospitalization. Selection of data inputs for this model was based on the Caprini and Wells models, which incorporate data elements such as Age, Sex, BMI, and ASA Physical Status [10–13]. In addition the model also incorporated additional data elements such as the type of surgery, length of surgery and associated comorbidities.

The patient level data was distributed across multiple sources (DxPx.txt, Elixahuser-CobMorb.txt, Height.txt), which were consolidated into a single R data-table. Patients were then either identified or labelled as having a VTE (positive) or not having a VTE (negative). Positive patients were further classified as having either a DVT or PE. Patients were identified as having a VTE by using the corresponding ICD10 codes. Because of the differences in patho-physiology and outcomes, two separate risk models were constructed, one for PE and one for DVT.

The data was heavily imbalanced with 265 positive VTE patients and 9370 negative patients. Therefore, the models had a strong potential to over-fit the data. In order to prevent this, various sampling methods were implemented in order to balance the dataset. Methods included were: up sampling, down sampling, Synthetic Minority Oversampling Technique (SMOTe), Random Oversampling Examples (ROSE) and a custom ensemble classifier that combined the previous four methods.

Up sampling is the method of randomly duplicating observations in the minority class to achieve an evenly balanced data set. Down sampling is the method of randomly selecting a subset of observations in the majority class to reach an evenly balanced data set. SMOTe uses machine learning techniques to create artificial data points in the data set. SMOTe accomplishes this by implementing a K-Nearest Neighbor (KNN) algorithm to map all the observations into sets of clusters, and then develops

artificial data points using inference of an observation and its closest nearest neighbors. ROSE similarly develops artificial data points, however instead of a machine learning approach, ROSE uses underlying statistical information to develop data points. ROSE accomplishes this by creating a probability distribution of observations from both classes, and then extracting samples from the distribution to develop artificial data. Finally, a combination of Up, Down, SMOTe, and ROSE sampling methods, called the Ensemble Sampling Method, was tested.

Four different classifiers were tested to determine the best VTE Risk Prediction Model: Random Forest (RF), Generalized Linear Models (GLM), Support Vector Machines (SVM), and Gradient Boosting Machines (GBM). GLM is the standard approach that was implemented first. Random Forest and GBM were then implemented after researching their effectiveness in predicting clinical infections in other clinical papers [16, 17]. However, it became apparent after a couple of tests that a linear classifier such as GLM performed better than the RF and GBM, more linear classifiers were explored and the SVM linear classifier was implemented in the training process. The data was finally split into 75/25 testing and training subsets.

In order to benchmark the classifiers, four statistical properties of the classifiers were compared to determine the model classifier: Sensitivity, Specificity, AUC and Balanced Accuracy. Sensitivity, or True Positive Rate, is the proportion of correctly identified positive VTE patients to the actual number of positive VTE patients. Specificity, or True Negative Rate, is the proportion of correctly identified negative VTE patients to the actual number of negative VTE patients. AUC, or Area Underneath the ROC Curve, measures the ability of the classifier to distinguish between a positive VTE instance and a negative VTE instance, the higher the number the better the classifier is able to distinguish between the two instances. Balanced Accuracy is the number of correctly classified instances of VTE to the observed instances of VTE, calculated as the average of the Sensitivity and Specificity. Balanced accuracy differs from

normal accuracy as it removes any bias caused by an imbalanced class. Full statistical information including Positive Predictive Value (PPV), Negative Predictive Value and Mcnemar's Test P-Value are located in the Appendix I.

2.4 Real Time VTE Classification Model

The second goal was to develop a Real-Time VTE Classification Model to determine whether or not the patient is experiencing a VTE at the time of the assessment. This was accomplished by analyzing high-frequency physiological time-series data captured via instruments directly attached to the patient. This allowed the model to provide updated prediction of a patients VTE status throughout their ICU stay.

Current VTE diagnostic measures do not establish a precise disease onset time, as diagnosis is performed re-actively based on signs and symptoms rather than proactively. Standard diagnostic measures include a Computed Tomography (CT) with Intravenous (IV) contrast, an ultrasound duplex scan, or an echocardiography. The time stamps of these studies can provide an indication of disease onset time.

However scans can be ordered for multiple reasons, especially in surgical-ICUs, where clinicians routinely scan patients. The outcome or cause of the study is infrequently documented in clinical notes. Therefore, in order to infer that the study was for VTE, the study is typically succeeded by the administration of IV heparin or low molecular weight heparin. Thus for the purpose of the this study, it was assumed that the order of therapeutic heparin within 24 hours of a diagnostic study time stamp was representative of VTE treatment.

Applying this methodology, 51 VTE positive patients were identified with appropriate corresponding time stamps. Time stamps can be used to determine VTE positive windows, periods of times when the patients is experiencing the signs and symptoms of VTE, which are used as classification labels for model development. Data was

recorded on a minute to minute basis, as such time stamps are accurate to the nearest minute. Because of the low number of total observations for this section, both the PE and DVT cohorts were merged.

Some assumptions had to be made in order to determine proper VTE positive windows. Based on the knowledge of clinical workflows, a positive VTE window for a DVT patient is 24 hours before and after diagnosis time, but the positive VTE window for a PE patient is 6 hours before and after diagnosis time. This is because PE is a more life threatening condition, and as such the response to an order for the exam and the initiation of therapy after a diagnostic exam are typically much faster.

The six physiological markers in the PTS data set are Arterial Blood Pressure Systolic, Arterial Blood Pressure Diastolic, Arterial Blood Pressure Mean, Respiratory Rate, Heart Rate, and Oxygen Saturation Level (SPO2). In order to consolidate the time series data set, the R tsfeatures package was used [15]. This package extracted 16 time series statistical features physiological per marker resulting in a total of 96 features.

Subsequently, a classification model was developed that would determines if a patient is experiencing a VTE based previously correlated observations. Classifiers such as Random Forest, K-Nearest Neighbors (KNN), and Naive Bayes (NB), were finally selected based on previous literature in addition to its training performance. Random Forest has shown promise in analyzing time series information for detecting Alzheimer's disease [18], while K-NN has been effectively implemented in analyzing ECG data to determine abnormal brain activity [19]. Naive Bayes was selected not only for its promise in analyzing clinical time series data [20], but also its effectiveness in predicting heart disease [21]. Similar to the VTE Risk Prediction Model, classifiers were benchmarked by their specificity, sensitivity, AUC and balanced accuracy.

Chapter 3

Results

In order to determine the best VTE Risk Prediction Model, four different classifiers were tested, Random Forest, Support Vector Machines, Generalized Linear Models, and Gradient Boosting Machines. Subsequently, to determine the best Real Time VTE Classification Model, three different classifiers were tested, Naive Bayes, K-Nearest Neighbors and Random Forest.

3.1 VTE Risk Prediction

The VTE Risk Prediction Model was split into two sub-models: DVT Risk Prediction Model and PE Risk Prediction Model.

3.1.1 DVT Risk Prediction Model

3.1.1.1 Training

Table 3-1 shows the number of positive DVT patients and negative DVT patients for the each of the different sampling methods.

Table 3-1. DVT Sampling Statistics

DVT Sampling Statistics		
Sampling Technique	Positive	Negative
No Sampling	134	7093
Up Sampling	7093	7093
Down Sampling	134	134
SMOTe	402	536
ROSE	3580	3647
Ensemble	2862	2364

The results for No sampling, Up sampling, and Down sampling are previously defined. The SMOTe and ensemble techniques led to a decrease in the total number of observations, while the ROSE technique yielded the same number of overall observations.

Table 3-2 and Figure 3-1 details the statistics and ROC curve of the best performing sampling method for each classifier, respectively. Training statistics and ROC curve were calculated for the in sample population. The GBM ensemble classifier was the best training model. More detailed statistics and ROC Curves for all classifiers are listed in Appendix I and Appendix II.

Table 3-2. DVT Training Results

DVT Training Results					
Classifier	Sampling Method	Sensitivity	Specificity	AUC	Balanced Accuracy
GLM	Up	0.708	0.560	0.715	0.634
SVM	Up	0.734	0.783	0.831	0.756
GBM	Ensemble	0.844	0.980	0.965	0.912
RF	Up	0.823	0.908	0.951	0.866

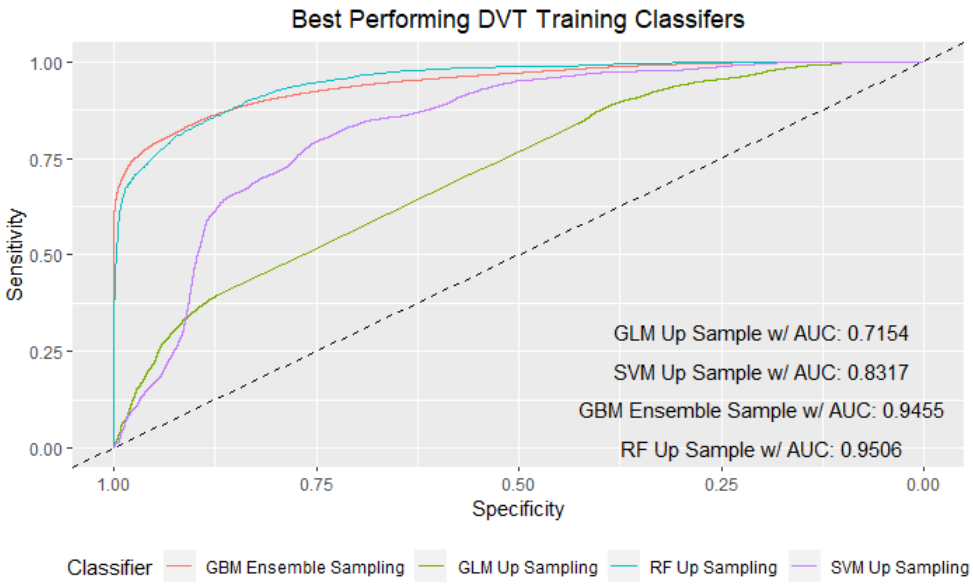

Figure 3-1. Best Performing DVT Training Classifiers

3.1.1.2 Testing

The model was tested on a previous withheld out of sample subset population, which had 44 positive and 2364 negative DVT patients. Table 3-3 and Figure 3-2 details the statistics and ROC curve for the best performing sampling method for each classifier. The SVM classifier with ensemble sampling was the best testing classifier. Test statistics and ROC curves for each tested classifier are available in Appendix I and Appendix II.

Table 3-3. DVT Testing Results

DVT Testing Results					
Classifier	Sampling Method	Sensitivity	Specificity	AUC	Balanced Accuracy
GLM	ROSE	0.522	0.767	0.7074	0.645
SVM	Ensemble	0.590	0.725	0.6721	0.659
GBM	Down	0.590	0.622	0.6743	0.606
RF	Down	0.431	0.811	0.698	0.621

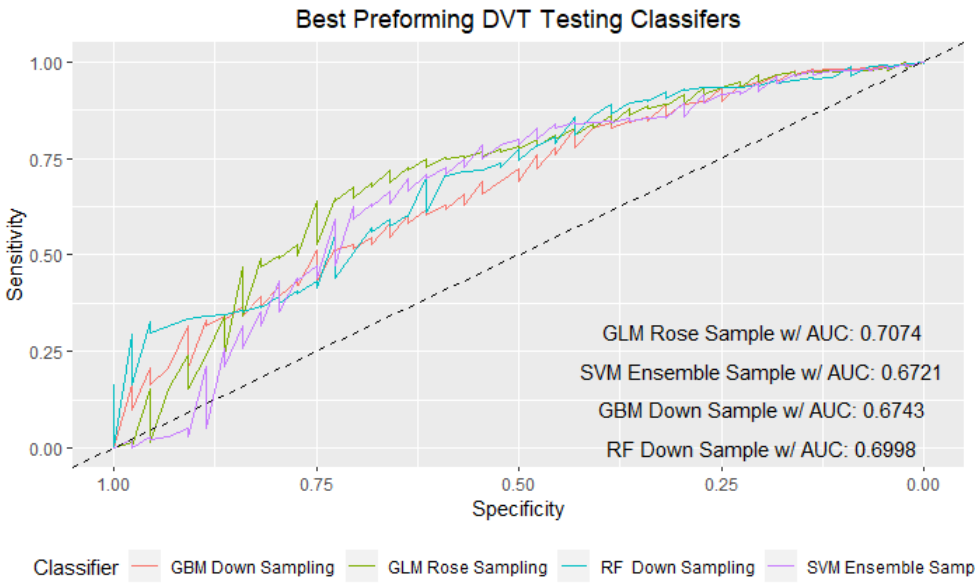

Figure 3-2. Best Performing DVT Testing Classifiers

3.1.1.3 Feature Importance

Table 3-4 indicates the top three ranked features for each DVT classifier. Feature Importance was calculated through the use of the R varimp function in the caret package. Overall, weight loss was a vital factor in predicting DVT prior to admissions, with three of the four classifiers ranking it as the most important feature. Full feature importance information is located in Appendix II.

Table 3-4. DVT Risk Prediction: Feature Importance

DVT Feature Importance Ranking				
Feature Rank	GLM	SVM	GBM	RF
1	Oncology	Weight Loss	Weight Loss	Weight Loss
2	PE History	ASA Physical Status	Surgery Length	Surgery Length
3	Ophthalmology	Surgery Length	Oculoplastics	PE history

3.1.2 PE Risk Prediction Model

3.1.2.1 Training

Table 3-5 is a table of the number of PE and Non-PE patients for each of the different sampling methods.

Table 3-5. PE Sampling Stats

PE Sampling Ratios		
Sampling Technique	Positive	Negative
No Sampling	98	7129
Up Sampling	7129	7129
Down Sampling	98	98
SMOTe	294	392
ROSE	3690	3537
Ensemble	3736	3168

The results for No sampling, Up sampling, and Down sampling are previously defined. The SMOTe and ensemble techniques led to a decrease in the total number of observations, while the ROSE technique yielded the same number of overall observations.

Table 3-6 and Figure 3-3 display the statistics and ROC curve for the best performing sampling method for each classifier, respectively. Training statistics and ROC curves were calculated using the in sample population. The GBM SMOTe and RF ROSE classifiers both were the best performing classifiers for this section. Further statistical information and ROC curves,for all classifiers are located in the Appendix I and Appendix II.

Table 3-6. PE Training Results

PE Training Results					
Classifier	Sampling Method	Sensitivity	Specificity	AUC	Balanced Accuracy
GLM	Up	0.480	0.821	0.736	0.650
SVM	Up	0.840	0.753	0.844	0.797
GBM	Smote	1.000	1.000	1.000	1.000
RF	Rose	1.000	1.000	1.000	1.000

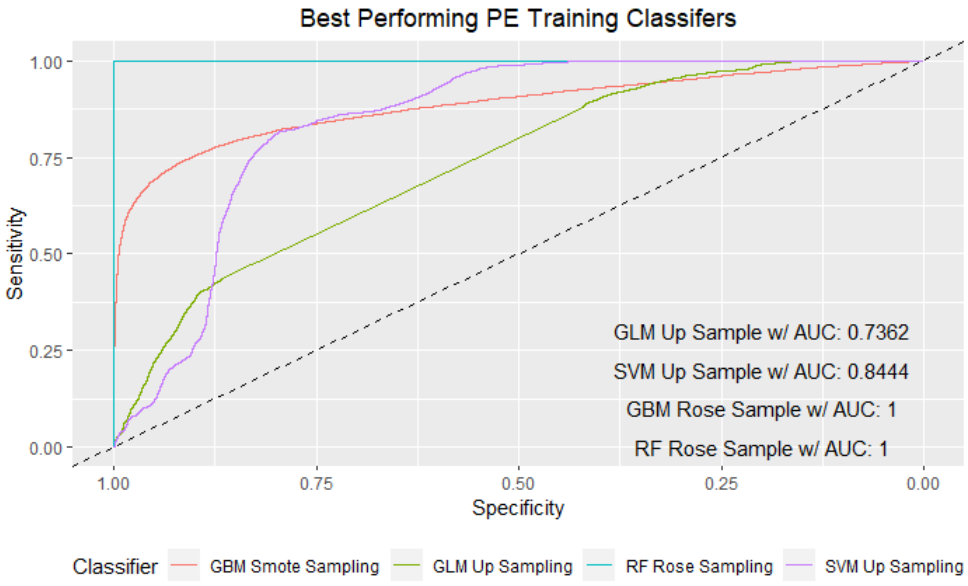

Figure 3-3. Best Performing PE Training ROC Curve Classifiers

3.1.2.2 Testing

The classifiers were tested on the withheld out of sample population of 32 positive and 2376 negative PE patients. Table 3-7 and Figure 3-4 shows the statistics and ROC curve for the best performing sampling methods per classifier. Overall the best performing classifier was the GBM classifier with down sampling. Statistics and ROC curves for all classifiers and sampling methods can be found in Appendix I and Appendix II.

Table 3-7. PE Testing Results

PE Testing Results					
Classifier	Sampling Method	Sensitivity	Specificity	AUC	Balanced Accuracy
GLM	Ensemble	0.625	0.627	0.652	0.626
SVM	Ensemble	0.562	0.683	0.682	0.623
GBM	Down	0.687	0.558	0.658	0.623
RF	Down	0.343	0.800	0.680	0.572

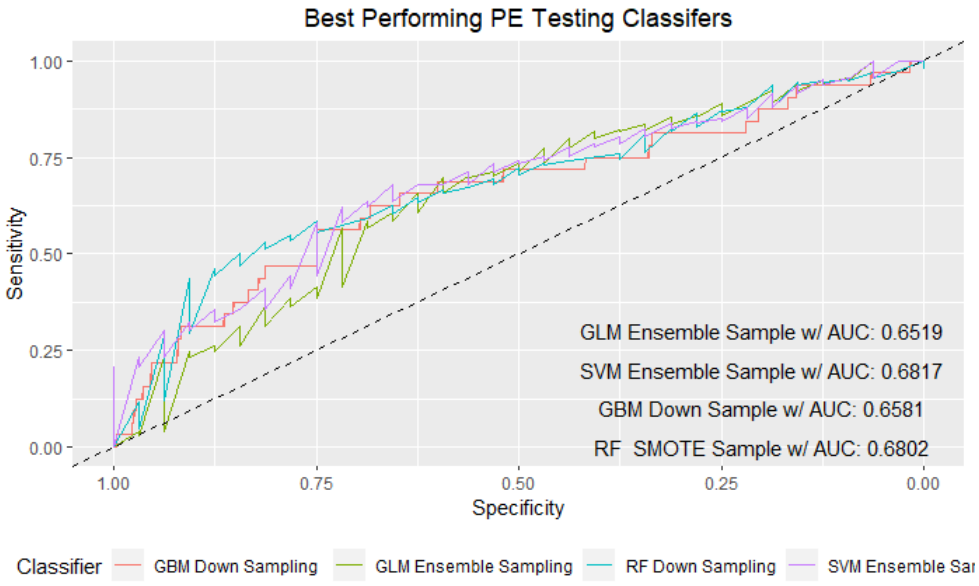

Figure 3-4. Best Performing PE Testing ROC Curve Classifiers

3.1.2.3 Feature Importance

Table 3-8 are the top three ranked features for each PE classifier. Feature importance was calculated through the varImp function in the R caret package. Overall, surgery length played a vital role in predicting VTE, being top feature in two different classifiers. Full feature importance information is available in the Appendix II.

Table 3-8. PE Risk Prediction: Feature Importance

PE Feature Importance Ranking				
Feature Rank	GLM	SVM	GBM	RF
1	PE History	White Caucasian	Surgery Length	Surgery Length
2	Orthopedics	Weight	Never Smoker	Peripheral vascular disease
3	Ophthalmology	Peripheral vascular Diesease	Gastrointestinal (DEPT)	Neuro spine surgery

3.2 Real-time VTE Classification Model

3.2.1 VTE

3.2.1.1 Training

Table 3-9 and Figure 3-5 detail the training performance and ROC curves of the three classifiers trained for Real Time VTE Classification Model. Training performance and ROC curves are calculated on the in sample population. The best performing training classifier was the Random Forest classifier.

Table 3-9. VTE Real Time Training Results

VTE Real Time Training Results				
Classifier	Sensitivity	Specificity	AUC	Balanced Accuracy
K-NN	0.933	0.705	0.858	0.820
Naive Bayes	0.571	0.892	0.903	0.732
Random Forest	0.771	0.982	0.985	0.876

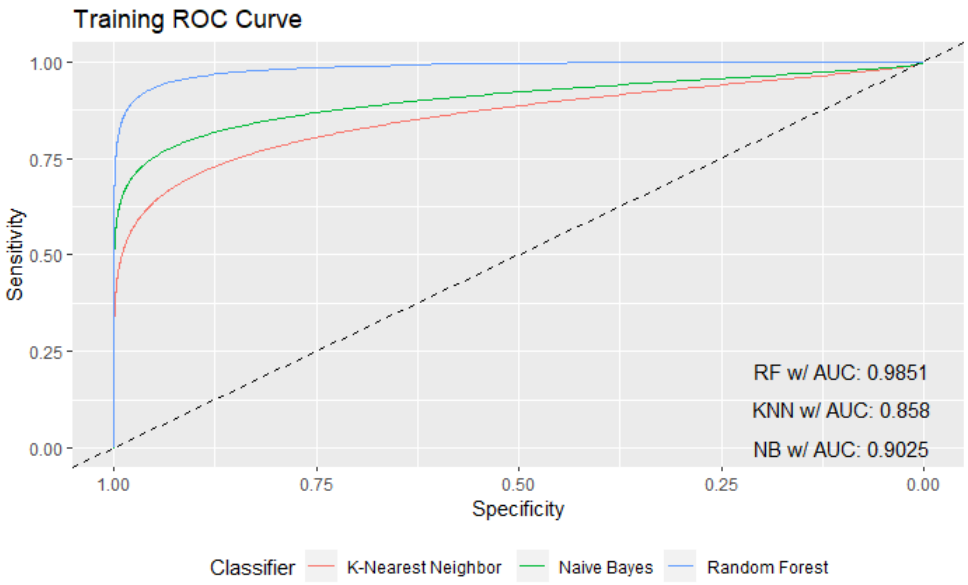

Figure 3-5. Real Time VTE Training ROC Curves

3.2.1.2 Testing

Classifiers were tested on a previously withheld out of sample population. Table 3-10 and Figure 3-6 details the testing performance and ROC curves of the three classifiers tested for Real Time VTE Classification Model. The best performing classifier in the testing phase was the Naive Bayes classifier.

Table 3-10. VTE Real Time Testing Results

VTE Real Time Testing Results				
Classifier	Sensitivity	Specificity	AUC	Balanced Accuracy
K-NN	1.000	0.500	0.749	0.750
Naive Bayes	1.000	0.900	0.947	0.950
Random Forest	0.667	0.900	0.913	0.783

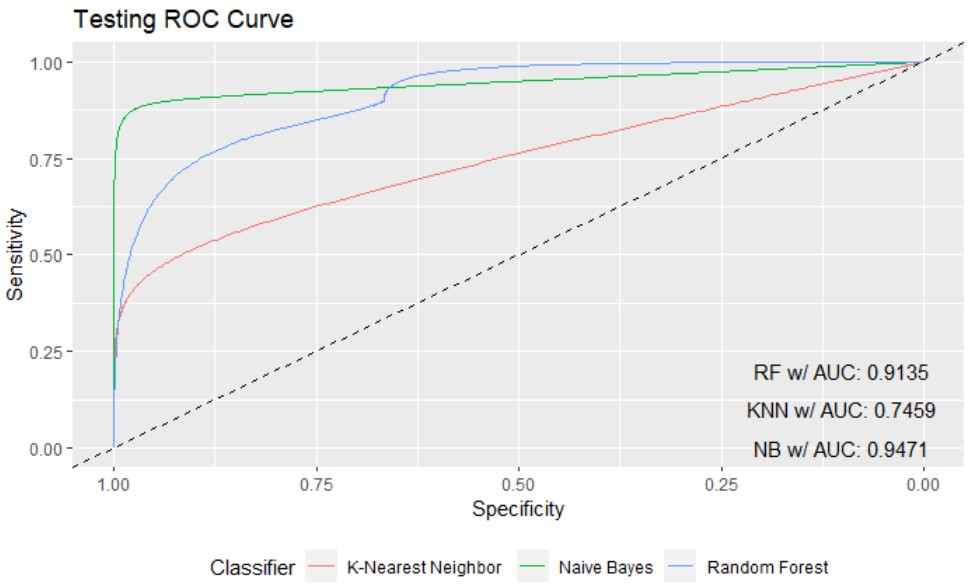

Figure 3-6. Real Time VTE Testing ROC Curves

3.2.1.3 Feature Importance

Table 3-11 detail top three ranked features per classifier Feature importance was calculated using the varImp function found in the R caret package. Overall, the most important physiological time series variable was Respiratory Rate, with all three models ranking it as the top feature. More detailed feature importance information can be found in Appendix II

Table 3-11. VTE Real Time Classification: Feature Importance

VTE Feature Importance Ranking			
Feature Rank	KNN	RF	NB
1	Respiratory Rate (Acf)	Respiratory Rate (Acf)	Respiratory Rate (Acf)
2	Respiratory Rate (Entropy)	Respiratory Rate (Entropy)	Respiratory Rate (Entropy)
3	Respiratory Rate (Spike)	Respiratory Rate (Spike)	Respiratory Rate (Spike)
4	Oxygen Saturation (Spike)	Oxygen Saturation (Acf)	Oxygen Saturation (Spike)

Chapter 4

Discussion

The importance of preventing and diagnosing VTE has been highlighted by numerous public health agencies including the Surgeon General of the United States [1], the National Institutes of Health, and the National Clinical Guideline Center (UK) [22]. VTE is both many times more prevalent and morbid in the critically ill than in hospitalized patients or the general public [23–26]. In addition, it is well recognized that the incidence of VTE is increased by surgery. In spite of this need, there are no highly specific and sensitive tools for assessing which patients are at risk for developing a VTE while in recovery in the surgical ICU. Thus, it was postulated that training a machine algorithm with a very wide set of critical care patients data could improve on current VTE risk models.

To accomplish this, two separate VTE models were constructed, a VTE Risk Prediction Model and a Real Time VTE Classification Model. The VTE Risk Prediction Model was further segmented into a DVT Risk Prediction Model and a PE Risk Prediction Model. For the DVT Risk Prediction Model training phase, the best performing classifier was the GBM with Ensemble sampling boasting the following metics: sensitivity of 0.844, specificity of 0.980, AUC of 0.965 and balanced accuracy of 0.912. However in the testing phase the best performing classifier was GBM with down sampling boasting following metrics: sensitivity of 0.590, specificity of 0.725, AUC of 0.6721 and balanced accuracy of 0.659. A possibility as to why there is a discrepancy

between testing and training is due to artificial data observations introduced in various sampling methods, which are easier to classify then actual observations. Furthermore, models perform better on training datasets than testing datasets because models built on training datasets and are much better optimized for it. Meanwhile, in the PE Risk Prediction Mode training phase, the best performing was the both the GBM classifier with SMOTe sampling and RF classifier with ROSE sampling, boasting the following metrics: sensitivity of 1.000, specificity of 1.000, AUC of 1.000 and balanced accuracy 1.000. One possibility as to why these two classifiers had perfect accuracy is because of the sampling methods. Both SMOTe and ROSE implement artificial observations derived from machine learning models or probability distributions rather than true observations, and thus making it easier for the classifier to correlate. However, performance analyzing artificial observations is not direct correlation to analysis of true observations, which were used for the testing phase of the model. In the testing phase, the best performing classifier was the GBM classifier with down sampling, boasting the following metrics: sensitivity of 0.687, specificity of 0.558, AUC of 0.658, balanced accuracy of 0.623. In comparison, current VTE RAMs analyze thrombosis markers to discriminate between VTE and non-VTE in a critically ill patients boast the following metrics: sensitivity of 0.660, specificity of 0.606, and an AUC of 0.696 [13].

Furthermore, the Real Time VTE Classification Model, which analyzes high-frequency physiological time series data, was significantly better in detecting if a patient was experiencing a VTE than current Risk Assessment Models, including those that were tested in this study. This is the first time that disease onset and physiological time series data has been incorporated into a VTE analysis and potentially allows the model to be used as a diagnostic screening tool rather than as simple risk analysis tool. In the testing phase, the strongest classifier was the K-NN, with a sensitivity of 0.933, a specificity of 0.705, an AUC of 0.858 and a balanced accuracy of 0.820. Meanwhile, the Naive Bayes was the best tested classifier, boasting a sensitivity

of 1.000, sensitivity of 0.900, AUC of 0.947 and a balanced accuracy of 0.950. In conclusion, the results presented were promising as it indicated that the inclusion of real time physiological time series will significantly improve the performance over current VTE risk assessment models.

For this novel approach, we applied assumptions about clinical workflow to our interpretation of the physiological time series data. This allowed us to assign a window of time in which the diagnosis of VTE was likely to have been made in our retrospective PTS data. The selection of data elements was informed by existing models and expanded to include elements that were collected in the medical record. The models did not assign any predetermined weight to input features. The routine use of ultrasound for VTE screening or diagnosis in critically ill patients is not recommended because it is believed that it will result in complications from treatment of VTE [27]. As a result, many risk assessment models (RAMs) have been created with the goal of using patient risk stratification to guide appropriate pharmacologic VTE prophylaxis or diagnostic screening. The value of these RAMs in general and in specific patient populations remains at issue. For example, Greene et al compared the discrimination and calibration of 4 widely used VTE RAMs applied retrospectively to general medical patients and found that discrimination was poor for all models and concluded that the existing RAMs, "...are suboptimal and are deserving of further enquiry", especially in critical illness and surgery because these conditions increase the risk of developing VTE [12, 28]. Furthermore, while pharmacologic DVT prophylaxis does not appear to increase the risk of significant postoperative bleeding this risk continues to impact prophylaxis [29–32].

This new model incorporated features that are clinically associated with the increased risk of VTE and are included in existing RAMs. Among the many VTE RAMs, the Caprini score has been the best validated and examined in post-surgical patients [11, 33–35].The Caprini model applied consensus guidelines about VTE risk

to create a scoring system in which clinical and patient-related factors are weighted [36]. However, the inclusion of the Elixhauser comorbidity features in our model allows a broader and less biased description of a patient's clinical state [14]. In addition, the complexity and lack of specificity of Caprini and other scoring systems have limited their utility in post-operative surgical populations. This complexity may explain why physician calculations of the Caprini scores of surgical patients were found to be inaccurate when compared to a validated computer calculation [37]. Importantly, one study of the Caprini score in surgical ICU patients found that the VTE rates were higher in surgical ICU patients for the same scores and suggested that this is probably due to the presence of risk factors that are not accounted for in the scoring system [38]. The combination of universally available patient data and the automation of processing this data may add to the clinical utility of the RAMs described in this work. This new models also have the advantage of ordering the importance of features contributing to VTE in post-surgical critical care patients. This method, known as feature importance, ranks features based on the calculated weights of features determined at training. This gives insight on the decision-making process our model uses when determining if a patient is at risk for VTE, and allows us to compare our model with previous work. For example, Obi and colleagues performed a validation of the Caprini VTE RAM in Critically Ill Surgical Patients and determined that factors such as age, weight, BMI, presence of tumor, major surgery ($>$ 45 mins), history of DVT or PE and for female specifically, the use of oral contraceptives or pregnancy are important. Furthermore, a paper published by Wells detailing the risks associated with pulmonary embolisms found that patients with cancer, previous DVT or PE, or those who are immobilized due to surgery have increased risk of developing a PE. Subsequently,this aligned with our non-priori weighted model, which highly ranked weight, PE history and surgery length. However, it should be noted that these features list comparisons are not one to one due to differentiating criteria. Other models, such as Wells and Caprini, have

looked at previous surgery as a feature, whereas all of our subjects have had surgery. As such, many of the previous models may not be compatible with our research data. This speaks to the novelty of our model, as it attempts the more challenging endeavor of classifying patients in a highly prevalent VTE environment, that are already at a higher risk of developing VTE. As such our data-set was a collaboration of features partly from previous models, collected patient commodities and selected data related specific for surgeries.

There is variation in the ranked feature importance within the DVT and PE models, despite classifying on the same dataset. This is part in due because each classier has different methods to determine feature importance, which is calculated as a correlation between dependent and independent variables. For example, linear models such as GLM used the t-statistic test, T-Test, to determine feature ranking, however in contrast Random Forest model, determines feature importance by determining the maximum decrease in classification accuracy when the feature is excluded. More importantly, these models are fundamentally different implementing different methodology and algorithms to classify patients. This difference in approach lead to variances in the feature weight ranking among classifiers. Having models with different ranked features can provide insight into correlations between features and VTE probability that were previously unknown.

In order to improve the use of RAMs, new models have been developed to simplify data elements and condition labeling. For example, Mlaver and colleagues performed a multivariate regression of NSQIP data to create a 5 component RAM for preoperative risk assessment of surgical patients. The simple COBRA model created by these authors was highly sensitive but had low specificity for peri-operative VTE risk [39]. In our RAMs for DVT and PE we have generally increased the number of data categories and accordingly the number of potential data elements. However, these elements are required components of patient records (clinical and administrative). Thus, the RAMs

presented in this work do not require the bedside clinician to interpret the patient's condition as part of the RAM. In addition, like other statistical scoring systems, our model is not dependent on a priori factor weights but rather uses the existing data set to develop a non-biased model.

Existing RAMs also suffer from a comparative lack of specificity, especially when applied to surgical or critically ill patients. Fu and colleagues highlighted this issue in a retrospective study of 151 patients in which they found that 88% of patients who did not have VTE had a Caprini score that placed them in the high or highest risk categories which amounted to a test specificity of 17% [13]. Similarly, Xu et al found that in post-cancer surgery ICU patients only approximately 3% had "symptomatic" VTE but 99.5% had the highest risk Caprini score [40]. Several groups have attempted to improve the specificity of RAMS by incorporating thrombosis bio-marker data in their RAM models. Fu et al suggested that the risk assessment correlates closely to serum levels of thrombosis markers especially thrombomodulin and that these can improve test specificity [13]. Similarly, Wang et al found that increased D-Dimer levels on post-operative day 5 in patients who underwent thoracic tumor surgery were independently correlated with DVT [41].

While DVT and PE are collectively included in the diagnosis of VTE and are intimately related they are not identical conditions. For this reason we disassociated these two diagnoses for the purposes of creating novel RAMs. This disassociation has both practical and clinical advantages. First, our algorithms can theoretically achieve higher specificity by considering DVT and PE independently since the conditions that lead to each outcome are likely to be different. Second, since PE is less prevalent than DVT the class imbalance inherent in model creation can be better recognized and mitigated. Finally, since RAMs for VTE are used to principally to guide prophylactic therapy, understanding the risk of suffering a PE rather than a DVT may impact decisions about chemo prophylaxis.

In the second phase of this work, patients were classified as as being in the VTE time window through analysis of physiological time series data (PTS). Eventually such a model could be applied to perform real time risk scores by analyzing the PTS data. While, previous scoring systems have used the concept that VTE disease does perturb cardiopulmonary status, the inclusion of PTS data in our model is a significant departure from previous VTE risk and likelihood scoring systems [42–44]. Here, we hypothesized that evidence of VTE is embedded within the PTS signals and that these may be discovered using advanced statistical techniques. We chose to use the twenty-four and six hour time windows around the clinical diagnosis of a DVT or PE, respectively, based on our perceptions of clinical workflows and the time to reach therapeutic goals with anticoagulants. Using this data we were able to create a Naïve Bayes machine learning model for VTE that has a very high accuracy and AUC for the ROC.

Clinical risk assessment for VTE using Artificial Intelligence in the form of neural networks has recently shown promise. For example, the Oxford Neural Network (ONN) is a DVT risk assessment model built on an artificial neural network using data of patients referred for DVT evaluation to an outpatient thrombosis clinic [10], The input layer of the ONN includes the data elements for Wells' criteria and the patients' age and gender. The ONN retains very high sensitivity and importantly may also improve specificity since it excluded 37.5% of patients who would have undergone unnecessary ultrasound exam [10].

An Artificial Neural Network (ANN) for VTE in hospitalized patients was created by Qatawneh et al who applied 35 elements from the Caprini score to an ANN that was trained using the records of only 150 hospitalized patients [45].Each input neuron was encoded with a perceived weight before analysis to produce an overall agreement with manual Caprini risk scoring of 81% [45]. Similarly, Martins and colleagues used data from 261 in-patients who had previously suffered VTE and combined Principle

Component Analysis with ANN to create models for to evaluate the risk of recurrence that had an accuracy of 92.8% or greater [46].

There are several limitations to our work and some of them are related to the use of retrospective data for the diagnosis of VTE. The diagnoses of VTE in the RAMs that we created using static data are completely dependent on the use of ICD 10 codes. In a previous study using ICD 10 codes as a marker of postoperative VTE their positive predictive value (PPV) was only between 44 – 48% [47]. This low PPV based on ICD codes could explain the lower than expected VTE rate of 2.8% in our patient cohort. Our model for PTS data used the combination of an ICD code for VTE in combination with a diagnostic study and the initiation of anticoagulant therapy. The coupling of ICD codes with diagnostic studies has been previously demonstrated to be both sensitive and specific [48]. In our data s we can't know the number of undetected or unaccounted VTE events. Undetected VTEs occur when a patient with an occult VTE does not undergo a diagnostic study while unaccounted VTEs can occur because of administrative coding deficiencies. In addition, by adding the requirement in the PTS data model that a patient initiate anticoagulant therapy we exclude the possibility that a patient has a VTE but that anticoagulation is contraindicated. The study is also limited by the relatively low number of VTE events which resulted in the class imbalance that we treated with sampling methods. Such treatments can result in over fitting of data in machine learning models. Finally, this study was conducted at a single, academic, tertiary hospital. Approaches to VTE prophylaxis and diagnosis are likely to vary significantly between healthcare institutions and future study will be needed to determine if the models described in this work can be used at other locations.

Chapter 5

Conclusion

The proposed model helps to address a serious issue critical care patients and doctors face, as Venous Thromboembolism is serious disease with life threatening consequences. The proposed system provides an additional layer of screening in order to assist clinicians in determining if the patient is at risk of developing a VTE. Currently, there is no standard for VTE risk assessment for critical care patients, and patients are screened for various reasons under various different circumstances. The lack of standard risk assessment procedure can lead to missed disease diagnosis which can be deadly for the patient. The proposed system is a two part model; the first part VTE Risk Prediction Model, a model predict the risk of a patient developing a VTE prior to entrance to the ICU and a; Real Time VTE Classification: a model that provides real time updates to the risk by analyzing high frequency physiological time series data. This cohesive system will help to provide a basis for clinicians to use when they are faced with the critical decision of determining if a patient is experienci ng a VTE. Furthermore, this system will monitor the patients VTE status even when support staff such as clinicians and nurses are not actively monitoring the patient. Overall, the results of this study were promising and showed that the analysis of the high-frequency real time physiological data significantly improves the models performance compared to existing RAMs and can be used as a diagnostic screening tool.

References

1. *The Surgeon General's Call to Action to Prevent Deep Vein Thrombosis and Pulmonary Embolism* English (Office of the Surgeon General (US), 2008).
2. Kyrle, P. A. & Eichinger, S. Deep vein thrombosis. *The Lancet* **365,** 1163–1174 (2005).
3. Walker, A. M. & Jick, H. Predictors of bleeding during heparin therapy. *Jama* **244,** 1209–1212 (1980).
4. Sheridan, D., Carter, C. & Kelton, J. G. A diagnostic test for heparin-induced thrombocytopenia. *Blood* **67,** 27–30 (1986).
5. Stuck, A. K., Spirk, D., Schaudt, J. & Kucher, N. Risk assessment models for venous thromboembolism in acutely ill medical patients. *Thrombosis and haemostasis* **117,** 801–808 (2017).
6. Cook, D. *et al.* Prevention and diagnosis of venous thromboembolism in critically ill patients: a Canadian survey. *Critical Care* **5,** 336 (2001).
7. Tripodi, A. D-dimer testing in laboratory practice. *Clinical chemistry* **57,** 1256–1262 (2011).
8. Ferroni, P. *et al.* Risk assessment for venous thromboembolism in chemotherapy-treated ambulatory cancer patients: a machine learning approach. *Medical Decision Making* **37,** 234–242 (2017).
9. Kim, J. S. *et al.* Examining the ability of artificial neural networks machine learning models to accurately predict complications following posterior lumbar spine fusion. *Spine* **43,** 853 (2018).
10. Willan, J., Katz, H. & Keeling, D. The use of artificial neural network analysis can improve the risk-stratification of patients presenting with suspected deep vein thrombosis. *British journal of haematology* **185,** 289–296 (2019).
11. Pannucci, C. J. *et al.* Validation of the Caprini risk assessment model in plastic and reconstructive surgery patients. *Journal of the American College of Surgeons* **212,** 105–112 (2011).
12. Greene, M. T. *et al.* Validation of risk assessment models of venous thromboembolism in hospitalized medical patients. *The American journal of medicine* **129,** 1001–e9 (2016).
13. Fu, Y., Liu, Y., Chen, S., Jin, Y. & Jiang, H. The combination of Caprini risk assessment scale and thrombotic biomarkers to evaluate the risk of venous thromboembolism in critically ill patients. *Medicine* **97** (2018).

14. Elixhauser, A., Steiner, C., Harris, D. R. & Coffey, R. M. Comorbidity measures for use with administrative data. *Medical care,* 8–27 (1998).

15. Yang, Y. & Hyndman, R. J. *tsfeatures: Introduction to the tsfeatures package* (2020).

16. Garc'ıa, M. N. M., Herráez, J. C. B., Barba, M. S. & Hernández, F. S. *Random forest based ensemble classifiers for predicting healthcare-associated infections in intensive care units* in *Distributed Computing and Artificial Intelligence, 13th International Conference* (2016), 303–311.

17. Zhang, Z., Zhao, Y., Canes, A., Steinberg, D., Lyashevska, O., *et al.* Predictive analytics with gradient boosting in clinical medicine. *Annals of translational medicine* **7** (2019).

18. Moore, P., Lyons, T., Gallacher, J. & Initiative, A. D. N. Random forest prediction of Alzheimer's disease using pairwise selection from time series data. *PloS one* **14,** e0211558 (2019).

19. Chaovalitwongse, W. A., Fan, Y.-J. & Sachdeo, R. C. On the time series k-nearest neighbor classification of abnormal brain activity. *IEEE Transactions on Systems, Man, and Cybernetics-Part A: Systems and Humans* **37,** 1005–1016 (2007).

20. Van der Heijden, M., Velikova, M. & Lucas, P. J. Learning Bayesian networks for clinical time series analysis. *Journal of biomedical informatics* **48,** 94–105 (2014).

21. Pattekari, S. A. & Parveen, A. Prediction system for heart disease using Naıve Bayes. *International Journal of Advanced Computer and Mathematical Sciences* **3,** 290–294 (2012).

22. Centre–Acute, N. C. G. & UK, C. C. Venous thromboembolism: Reducing the risk of venous thromboembolism (deep vein thrombosis and pulmonary embolism) in patients admitted to hospital (2010).

23. Patel, R. *et al.* for the Burden of Illness in Venous Thrombo Embolism in Critical Care (BITEC) Study Investigators; Canadian Critical Care Trials Group: Burden of illness in venous thromboembolism in critical care: a multicenter observational study. *J Crit Care* **20,** 341–347 (2005).

24. Attia, J. *et al.* Deep vein thrombosis and its prevention in critically ill adults. *Archives of Internal Medicine* **161,** 1268–1279 (2001).

25. For the Canadian Critical Care Trials Group, P. I., the Australian & Group, N. Z. I. C. S. C. T. Dalteparin versus unfractionated heparin in critically ill patients. *New England Journal of Medicine* **364,** 1305–1314 (2011).

26. Hirsch, D. R., Ingenito, E. P. & Goldhaber, S. Z. Prevalence of deep venous thrombosis among patients in medical intensive care. *Jama* **274,** 335–337 (1995).

27. Ahmed, A. B., Koster, A., Lance, M., Faraoni, D., *et al.* European guidelines on perioperative venous thromboembolism prophylaxis: cardiovascular and thoracic surgery. *European Journal of Anaesthesiology| EJA* **35,** 84–89 (2018).

28. Cook, D. J., Crowther, M. A., Meade, M. O., Douketis, J., *et al.* Prevalence, incidence, and risk factors for venous thromboembolism in medical-surgical intensive care unit patients. *Journal of critical care* **20,** 309–313 (2005).

29. Leonardi, M. J., McGory, M. L. & Ko, C. Y. The rate of bleeding complications after pharmacologic deep venous thrombosis prophylaxis: a systematic review of 33 randomized controlled trials. *Archives of Surgery* **141,** 790–799 (2006).

30. Persson, G., Strömberg, J., Svennblad, B. & Sandblom, G. Risk of bleeding associated with use of systemic thromboembolic prophylaxis during laparoscopic cholecystectomy. *British journal of surgery* **99,** 979–986 (2012).

31. Pannucci, C. J., Swistun, L., MacDonald, J. K., Henke, P. K. & Brooke, B. S. Individualized venous thromboembolism risk stratification using the 2005 Caprini score to identify the benefits and harms of chemoprophylaxis in surgical patients: a meta-analysis. *Annals of surgery* **265,** 1094–1103 (2017).

32. Pannucci, C. J. *et al.* The effect of post-operative enoxaparin on risk for re-operative hematoma. *Plastic and reconstructive surgery* **129,** 160 (2012).

33. Gould, M. K. *et al.* Prevention of VTE in nonorthopedic surgical patients: antithrombotic therapy and prevention of thrombosis: American College of Chest Physicians Evidence-Based Clinical Practice Guidelines. *Chest* **141,** e227S–e277S (2012).

34. Bahl, V. *et al.* A validation study of a retrospective venous thromboembolism risk scoring method. *Annals of surgery* **251,** 344–350 (2010).

35. Shuman, A. G. *et al.* Stratifying the risk of venous thromboembolism in otolaryngology. *Otolaryngology–Head and Neck Surgery* **146,** 719–724 (2012).

36. Motykie, G. D. *et al.* A guide to venous thromboembolism risk factor assessment. *Journal of thrombosis and thrombolysis* **9,** 253–262 (2000).

37. Pannucci, C. J. *et al.* Inadequate venous thromboembolism risk stratification predicts venous thromboembolic events in surgical intensive care unit patients. *Journal of the American College of Surgeons* **218,** 898–904 (2014).

38. Obi, A. T. *et al.* Validation of the Caprini venous thromboembolism risk assessment model in critically ill surgical patients. *JAMA surgery* **150,** 941–948 (2015).

39. Mlaver, E., Lynde, G. C., Gallion, C., Sweeney, J. F. & Sharma, J. *Development of a Novel Preoperative Venous Thromboembolism Risk Assessment Model* 2020.

40. Wang, H.-Z. W. Incidence and risk assessment of venous thromboembolism in cancer patients admitted to intensive care unit for post-operative care. *Age* **61,** 74 (2018).

41. Wang, P. *et al.* Risk Factors and Clinical Significance of D-Dimer in the Development of Postoperative Venous Thrombosis in Patients with Lung Tumor. *Cancer Management and Research* **12,** 5169 (2020).

42. Wells, P. S. *et al.* Derivation of a simple clinical model to categorize patients probability of pulmonary embolism: increasing the models utility with the SimpliRED D-dimer. *Thrombosis and haemostasis* **83,** 416–420 (2000).

43. Le Gal, G. *et al.* Prediction of pulmonary embolism in the emergency department: the revised Geneva score. *Annals of internal medicine* **144,** 165–171 (2006).

44. Righini, M., Robert-Ebadi, H. & Le Gal, G. Diagnosis of acute pulmonary embolism. *Journal of Thrombosis and Haemostasis* **15,** 1251–1261 (2017).

45. Qatawneh, Z., Alshraideh, M., Almasri, N., Tahat, L. & Awidi, A. Clinical decision support system for venous thromboembolism risk classification. *Applied computing and informatics* **15,** 12–18 (2019).

46. Martins, T., Annichino-Bizzacchi, J., Romano, A. & Maciel Filho, R. Artificial neural networks for prediction of recurrent venous thromboembolism. *International journal of medical informatics* **141,** 104221 (2020).

47. White, R. H. *et al.* How valid is the ICD-9-CM based AHRQ patient safety indicator for postoperative venous thromboembolism? *Medical care,* 1237–1243 (2009).

48. Alotaibi, G. S., Wu, C., Senthilselvan, A. & McMurtry, M. S. The validity of ICD codes coupled with imaging procedure codes for identifying acute venous thromboembolism using administrative data. *Vascular medicine* **20,** 364–368 (2015).

Appendix I

Tables and Confusion Matricies

A. VTE Risk Prediction

A..1 DVT Models

A..1.1 GLM

Table I-1. GLM DVT No Sampling Confusion Matrix and Statistics

Confusion Matrix		
Prediction	Reference	
	Postive	Negative
Positive	0	0
Negative	44	2364
Test Statistics		
Statistic	Value	
Accuracy	0.982	
95% CI	(0.9755 0.9867)	
Balanced Accuracy	0.500	
Sensitivity	0.00	
Specificity	1.00	
Pos Pred Value	NaN	
Neg Pred Value	0.982	
Mcnemar's Test P-value	9.022e-11	

Table I-2. GLM DVT Up Sampling Confusion Matrix and Statistics

Confusion Matrix		
Prediction	Reference	
	Postive	Negative
Positive	21	519
Negative	23	1845
Test Statistics		
Statistic	Value	
Accuracy	0.775	
95% CI	(0.758 0.792)	
Balanced Accuracy	0.629	
Sensitivity	0.477	
Specificity	0.780	
Pos Pred Value	0.039	
Neg Pred Value	0.980	
Mcnemar's Test P-value	<2e-16	

Table I-3. GLM DVT Down Sampling Confusion Matrix and Statistics

Confusion Matrix		
Prediction	Reference	
	Postive	Negative
Positive	27	715
Negative	17	1649
Test Statistics		
Statistic	Value	
Accuracy	0.696	
95% CI	(0.677 0.714)	
Balanced Accuracy	0.656	
Sensitivity	0.613	
Specificity	0.698	
Pos Pred Value	0.036	
Neg Pred Value	0.990	
Mcnemar's Test P-value	<2e-16	

Table I-4. GLM DVT ROSE Sampling Confusion Matrix and Statistics

Confusion Matrix		
Prediction	Reference	
	Postive	Negative
Positive	23	550
Negative	21	1814
Test Statistics		
Statistic	Value	
Accuracy	0.7629	
95% CI	(0.754 0.779)	
Balanced Accuracy	0.645	
Sensitivity	0.522	
Specificity	0.767	
Pos Pred Value	0.040	
Neg Pred Value	0.989	
Mcnemar's Test P-value	<2e-16	

Table I-5. GLM DVT SMOTe Sampling Confusion Matrix and Statistics

Confusion Matrix		
Prediction	Reference	
	Postive	Negative
Positive	12	300
Negative	32	2064
Test Statistics		
Statistic	Value	
Accuracy	0.862	
95% CI	(0.848 0.876)	
Balanced Accuracy	0.573	
Sensitivity	0.273	
Specificity	0.873	
Pos Pred Value	0.038	
Neg Pred Value	0.984	
Mcnemar's Test P-value	<2e-16	

Table I-6. GLM DVT Ensemble Sampling Confusion Matrix and Statistics

Confusion Matrix		
Prediction	Reference	
	Postive	Negative
Positive	29	818
Negative	15	1546
Test Statistics		
Statistic	Value	
Accuracy	0.654	
95% CI	(0.635 0.673)	
Balanced Accuracy	0.656	
Sensitivity	0.659	
Specificity	0.654	
Pos Pred Value	0.034	
Neg Pred Value	0.990	
Mcnemar's Test P-value	<2e-16	

A..1.2 SVM Linaer Models

Table I-7. SVM DVT No Sampling Confusion Matrix and Statistics

Confusion Matrix		
	Reference	
Prediction	Postive	Negative
Positive	0	0
Negative	44	2364
Test Statistics		
Statistic	Value	
Accuracy	0.982	
95% CI	(0.975 0.987)	
Balanced Accuracy	0.500	
Sensitivity	0.000	
Specificity	1.00	
Pos Pred Value	NaN	
Neg Pred Value	0.982	
Mcnemar's Test P-value	9.022e-11	

Table I-8. SVM DVT Up Sampling Confusion Matrix and Statistics

Confusion Matrix		
	Reference	
Prediction	Postive	Negative
Positive	22	515
Negative	22	1849
Test Statistics		
Statistic	Value	
Accuracy	0.777	
95% CI	(0.759 0.794)	
Balanced Accuracy	0.641	
Sensitivity	0.500	
Specificity	0.782	
Pos Pred Value	0.041	
Neg Pred Value	0.988	
Mcnemar's Test P-value	<2e-16	

Table I-9. SVM DVT Down Sampling Confusion Matrix and Statistics

Confusion Matrix		
	Reference	
Prediction	Postive	Negative
Positive	28	817
Negative	16	1547
Test Statistics		
Statistic	Value	
Accuracy	0.654	
95% CI	(0.4 0.673)	
Balanced Accuracy	0.645	
Sensitivity	0.636	
Specificity	0.654	
Pos Pred Value	0.031	
Neg Pred Value	0.989	
Mcnemar's Test P-value	<2e-16	

Table I-10. SVM DVT ROSE Sampling Confusion Matrix and Statistics

Confusion Matrix		
	Reference	
Prediction	Postive	Negative
Positive	23	550
Negative	21	1814
Test Statistics		
Statistic	Value	
Accuracy	0.765	
95% CI	(0.747 0.781)	
Balanced Accuracy	0.645	
Sensitivity	0.522	
Specificity	0.769	
Pos Pred Value	0.040	
Neg Pred Value	0.988	
Mcnemar's Test P-value	<2e-16	

Table I-11. SVM DVT SMOTe Sampling Confusion Matrix and Statistics

Confusion Matrix		
	Reference	
Prediction	Postive	Negative
Positive	14	302
Negative	30	2062
Test Statistics		
Statistic	Value	
Accuracy	0.8621	
95% CI	(0.848 0.876)	
Balanced Accuracy	0.595	
Sensitivity	0.318	
Specificity	0.872	
Pos Pred Value	0.044	
Neg Pred Value	0.958	
Mcnemar's Test P-value	<2e-16	

Table I-12. SVM DVT Ensemble Sampling Confusion Matrix and Statistics

Confusion Matrix		
	Reference	
Prediction	Postive	Negative
Positive	26	649
Negative	18	1715
Test Statistics		
Statistic	Value	
Accuracy	0.723	
95% CI	(0.705 0.741)	
Balanced Accuracy	0.658	
Sensitivity	0.590	
Specificity	0.721	
Pos Pred Value	0.039	
Neg Pred Value	0.990	
Mcnemar's Test P-value	<2e-16	

A..1.3 GBM Models

Table I-13. GBM DVT No Sampling Confusion Matrix and Statistics

Confusion Matrix		
	Reference	
Prediction	Postive	Negative
Positive	0	0
Negative	44	2364
Test Statistics		
Statistic	Value	
Accuracy	0.982	
95% CI	(0.9755 0.9867)	
Balanced Accuracy	0.500	
Sensitivity	0.000	
Specificity	1.000	
Pos Pred Value	NaN	
Neg Pred Value	0.982	
Mcnemar's Test P-value	9.022e-11	

Table I-14. GBM DVT Up Sampling Confusion Matrix and Statistics

Confusion Matrix		
	Reference	
Prediction	Postive	Negative
Positive	20	368
Negative	24	1996
Test Statistics		
Statistic	Value	
Accuracy	0.837	
95% CI	(0.821 0.851)	
Balanced Accuracy	0.649	
Sensitivity	0.454	
Specificity	0.844	
Pos Pred Value	0.051	
Neg Pred Value	0.988	
Mcnemar's Test P-value	<2e-16	

Table I-15. GBM DVT Down Sampling Confusion Matrix and Statistics

Confusion Matrix		
	Reference	
Prediction	Postive	Negative
Positive	26	893
Negative	18	1471
Test Statistics		
Statistic	Value	
Accuracy	0.622	
95% CI	(0.602 0.641)	
Balanced Accuracy	0.606	
Sensitivity	0.599	
Specificity	0.622	
Pos Pred Value	0.018	
Neg Pred Value	0.987	
Mcnemar's Test P-value	<2e-16	

Table I-16. GBM DVT ROSE Sampling Confusion Matrix and Statistics

Confusion Matrix		
	Reference	
Prediction	Postive	Negative
Positive	44	2364
Negative	0	0
Test Statistics		
Statistic	Value	
Accuracy	0.018	
95% CI	(0.013 0.024)	
Balanced Accuracy	0.500	
Sensitivity	1.000	
Specificity	0.000	
Pos Pred Value	0.018	
Neg Pred Value	NaN	
Mcnemar's Test P-value	<2e-16	

Table I-17. GBM DVT SMOTe Sampling Confusion Matrix and Statistics

Confusion Matrix		
	Reference	
Prediction	Postive	Negative
Positive	7	139
Negative	37	2225
Test Statistics		
Statistic	Value	
Accuracy	0.963	
95% CI	(0.915 0.937)	
Balanced Accuracy	0.550	
Sensitivity	0.159	
Specificity	0.941	
Pos Pred Value	0.048	
Neg Pred Value	0.986	
Mcnemar's Test P-value	<2e-16	

Table I-18. GBM DVT Ensemble Sampling Confusion Matrix and Statistics

Confusion Matrix		
	Reference	
Prediction	Postive	Negative
Positive	11	201
Negative	33	2163
Test Statistics		
Statistic	Value	
Accuracy	0.902	
95% CI	(0.890 0.914)	
Balanced Accuracy	0.582	
Sensitivity	0.250	
Specificity	0.915	
Pos Pred Value	0.051	
Neg Pred Value	0.948	
Mcnemar's Test P-value	<2e-16	

A..1.4 Random Forest Models

Table I-19. RF DVT No Sampling Confusion Matrix and Statistics

Confusion Matrix		
	Reference	
Prediction	Postive	Negative
Positive	0	0
Negative	44	2364
Test Statistics		
Statistic	Value	
Accuracy	0.982	
95% CI	(0.9755 0.9867)	
Balanced Accuracy	0.500	
Sensitivity	0.000	
Specificity	1.000	
Pos Pred Value	NaN	
Neg Pred Value	0.982	
Mcnemar's Test P-value	9.022e-11	

Table I-20. RF Up Sampling Confusion Matrix and Statistics

Confusion Matrix		
	Reference	
Prediction	Postive	Negative
Positive	13	206
Negative	31	2158
Test Statistics		
Statistic	Value	
Accuracy	0.902	
95% CI	(0.889 0.913)	
Balanced Accuracy	0.604	
Sensitivity	0.295	
Specificity	0.912	
Pos Pred Value	0.059	
Neg Pred Value	0.985	
Mcnemar's Test P-value	<2e-16	

Table I-21. RF DVT Down Sampling Confusion Matrix and Statistics

Confusion Matrix		
	Reference	
Prediction	Postive	Negative
Positive	19	447
Negative	25	1917
Test Statistics		
Statistic	Value	
Accuracy	0.804	
95% CI	(0.788 0.820)	
Balanced Accuracy	0.621	
Sensitivity	0.431	
Specificity	0.810	
Pos Pred Value	0.041	
Neg Pred Value	0.987	
Mcnemar's Test P-value	<2e-16	

Table I-22. RF DVT ROSE Sampling Confusion Matrix and Statistics

Confusion Matrix		
	Reference	
Prediction	Postive	Negative
Positive	44	2364
Negative	0	0
Test Statistics		
Statistic	Value	
Accuracy	0.018	
95% CI	(0.013 0.024)	
Balanced Accuracy	0.500	
Sensitivity	1.000	
Specificity	0.000	
Pos Pred Value	0.018	
Neg Pred Value	NaN	
Mcnemar's Test P-value	<2e-16	

Table I-23. RF DVT SMOTe Sampling Confusion Matrix and Statistics

Confusion Matrix		
	Reference	
Prediction	Postive	Negative
Positive	1	12
Negative	43	2352
Test Statistics		
Statistic	Value	
Accuracy	0.977	
95% CI	(0.970 0.983)	
Balanced Accuracy	0.509	
Sensitivity	0.023	
Specificity	0.995	
Pos Pred Value	0.077	
Neg Pred Value	0.982	
Mcnemar's Test P-value	<2e-16	

Table I-24. RF DVT Ensemble Sampling Confusion Matrix and Statistics

Confusion Matrix		
	Reference	
Prediction	Postive	Negative
Positive	0	3
Negative	44	2361
Test Statistics		
Statistic	Value	
Accuracy	0.981	
95% CI	(0.974 0.986)	
Balanced Accuracy	0.499	
Sensitivity	0.000	
Specificity	0.998	
Pos Pred Value	0.000	
Neg Pred Value	0.981	
Mcnemar's Test P-value	<2e-16	

A..2 PE Models

A..2.1 GLM Models

Table I-25. GLM PE No Sampling Confusion Matrix and Statistics

Confusion Matrix		
	Reference	
Prediction	Postive	Negative
Positive	0	0
Negative	32	2376
Test Statistics		
Statistic	Value	
Accuracy	0.988	
95% CI	(0.981 0.990)	
Balanced Accuracy	0.500	
Sensitivity	0.000	
Specificity	1.000	
Pos Pred Value	0.NaN	
Neg Pred Value	0.988	
Mcnemar's Test P-value	4.251e-8	

Table I-26. GLM PE Up Sampling Confusion Matrix and Statistics

Confusion Matrix		
	Reference	
Prediction	Postive	Negative
Positive	0	0
Negative	32	2376
Test Statistics		
Statistic	Value	
Accuracy	0.988	
95% CI	(0.981 0.990)	
Balanced Accuracy	0.500	
Sensitivity	0.000	
Specificity	1.000	
Pos Pred Value	0.NaN	
Neg Pred Value	0.988	
Mcnemar's Test P-value	<2e-16	

Table I-27. GLM PE Down Sampling Confusion Matrix and Statistics

Confusion Matrix		
	Reference	
Prediction	Postive	Negative
Positive	20	930
Negative	12	1446
Test Statistics		
Statistic	Value	
Accuracy	0.608	
95% CI	(0.589 0.6248)	
Balanced Accuracy	0.616	
Sensitivity	0.625	
Specificity	0.608	
Pos Pred Value	0.021	
Neg Pred Value	0.991	
Mcnemar's Test P-value	<2e-16	

Table I-28. GLM PE ROSE Sampling Confusion Matrix and Statistics

Confusion Matrix		
	Reference	
Prediction	Postive	Negative
Positive	16	711
Negative	16	1665
Test Statistics		
Statistic	Value	
Accuracy	0.698	
95% CI	(0.679 0.716)	
Balanced Accuracy	0.600	
Sensitivity	0.500	
Specificity	0.700	
Pos Pred Value	0.022	
Neg Pred Value	0.990	
Mcnemar's Test P-value	<2e-16	

Table I-29. GLM PE SMOTe Sampling Confusion Matrix and Statistics

Confusion Matrix		
	Reference	
Prediction	Postive	Negative
Positive	8	321
Negative	24	2055
Test Statistics		
Statistic	Value	
Accuracy	0.856	
95% CI	(0.842 0.870)	
Balanced Accuracy	0.557	
Sensitivity	0.250	
Specificity	0.864	
Pos Pred Value	0.024	
Neg Pred Value	0.988	
Mcnemar's Test P-value	<2e-16	

Table I-30. GLM PE Ensemble Sampling Confusion Matrix and Statistics

Confusion Matrix		
	Reference	
Prediction	Postive	Negative
Positive	20	885
Negative	21	1491
Test Statistics		
Statistic	Value	
Accuracy	0.628	
95% CI	(0.608 0.646)	
Balanced Accuracy	0.6226	
Sensitivity	0.625	
Specificity	0.627	
Pos Pred Value	0.022	
Neg Pred Value	0.996	
Mcnemar's Test P-value	<2e-16	

A..2.2 SVM Linear

Table I-31. SVM PE No Sampling Confusion Matrix and Statistics

Confusion Matrix		
	Reference	
Prediction	Postive	Negative
Positive	0	0
Negative	32	2376
Test Statistics		
Statistic	Value	
Accuracy	0.988	
95% CI	(0.981 0.991)	
Balanced Accuracy	0.500	
Sensitivity	0.000	
Specificity	1.000	
Pos Pred Value	NaN	
Neg Pred Value	0.986	
Mcnemar's Test P-value	4.251e-8	

Table I-32. SVM PE Up Sampling Confusion Matrix and Statistics

Confusion Matrix		
	Reference	
Prediction	Postive	Negative
Positive	16	628
Negative	16	1748
Test Statistics		
Statistic	Value	
Accuracy	0.733	
95% CI	(0.714 0.750)	
Balanced Accuracy	0.618	
Sensitivity	0.500	
Specificity	0.735	
Pos Pred Value	0.024	
Neg Pred Value	0.990	
Mcnemar's Test P-value	<2e-16	

Table I-33. SVM PE Down Sampling Confusion Matrix and Statistics

Confusion Matrix		
	Reference	
Prediction	Postive	Negative
Positive	18	836
Negative	14	1540
Test Statistics		
Statistic	Value	
Accuracy	0.647	
95% CI	(0.627 0.666)	
Balanced Accuracy	0.605	
Sensitivity	0.562	
Specificity	0.641	
Pos Pred Value	0.021	
Neg Pred Value	0.990	
Mcnemar's Test P-value	<2e-16	

Table I-34. SVM PE ROSE Sampling Confusion Matrix and Statistics

Confusion Matrix		
	Reference	
Prediction	Postive	Negative
Positive	16	647
Negative	24	1729
Test Statistics		
Statistic	Value	
Accuracy	0.724	
95% CI	(0.706 0.742)	
Balanced Accuracy	0.613	
Sensitivity	0.500	
Specificity	0.727	
Pos Pred Value	0.024	
Neg Pred Value	0.990	
Mcnemar's Test P-value	<2e-16	

Table I-35. SVM PE SMOTe Sampling Confusion Matrix and Statistics

Confusion Matrix		
	Reference	
Prediction	Postive	Negative
Positive	9	387
Negative	23	1989
Test Statistics		
Statistic	Value	
Accuracy	0.827	
95% CI	(0.814 0.844)	
Balanced Accuracy	0.559	
Sensitivity	0.281	
Specificity	0.837	
Pos Pred Value	0.022	
Neg Pred Value	0.988	
Mcnemar's Test P-value	<2e-16	

Table I-36. SVM PE Ensemble Sampling Confusion Matrix and Statistics

Confusion Matrix		
	Reference	
Prediction	Postive	Negative
Positive	18	751
Negative	14	1625
Test Statistics		
Statistic	Value	
Accuracy	0.682	
95% CI	(0.663 0.701)	
Balanced Accuracy	0.623	
Sensitivity	0.563	
Specificity	0.683	
Pos Pred Value	0.023	
Neg Pred Value	0.991	
Mcnemar's Test P-value	<2e-16	

A..2.3 GBM Models

Table I-37. GBM PE No Sampling Confusion Matrix and Statistics

Confusion Matrix		
	Reference	
Prediction	Postive	Negative
Positive	0	0
Negative	32	2376
Test Statistics		
Statistic	Value	
Accuracy	0.987	
95% CI	(0.981 0.991)	
Balanced Accuracy	0.500	
Sensitivity	0.000	
Specificity	1.000	
Pos Pred Value	NaN	
Neg Pred Value	0.987	
Mcnemar's Test P-value	4.251e-18	

Table I-38. GBM PE Up Sampling Confusion Matrix and Statistics

Confusion Matrix		
	Reference	
Prediction	Postive	Negative
Positive	12	340
Negative	20	2036
Test Statistics		
Statistic	Value	
Accuracy	0.851	
95% CI	(0.836 0.865)	
Balanced Accuracy	0.615	
Sensitivity	0.375	
Specificity	0.856	
Pos Pred Value	0.034	
Neg Pred Value	0.990	
Mcnemar's Test P-value	<2e-16	

Table I-39. GBM PE Down Sampling Confusion Matrix and Statistics

Confusion Matrix		
	Reference	
Prediction	Postive	Negative
Positive	22	1048
Negative	10	1328
Test Statistics		
Statistic	Value	
Accuracy	0.561	
95% CI	(0.541 0.581)	
Balanced Accuracy	0.623	
Sensitivity	0.687	
Specificity	0.558	
Pos Pred Value	0.020	
Neg Pred Value	0.992	
Mcnemar's Test P-value	<2e-16	

Table I-40. GBM PE ROSE Sampling Confusion Matrix and Statistics

Confusion Matrix		
	Reference	
Prediction	Postive	Negative
Positive	32	2376
Negative	0	0
Test Statistics		
Statistic	Value	
Accuracy	0.013	
95% CI	(0.009 0.019)	
Balanced Accuracy	0.500	
Sensitivity	1.000	
Specificity	0.000	
Pos Pred Value	0.013	
Neg Pred Value	NaN	
Mcnemar's Test P-value	<2e-16	

Table I-41. GBM PE SMOTe Sampling Confusion Matrix and Statistics

Confusion Matrix		
	Reference	
Prediction	Postive	Negative
Positive	7	177
Negative	25	2199
Test Statistics		
Statistic	Value	
Accuracy	0.916	
95% CI	(0.904 0.927)	
Balanced Accuracy	0.572	
Sensitivity	0.219	
Specificity	0.925	
Pos Pred Value	0.038	
Neg Pred Value	0.988	
Mcnemar's Test P-value	<2e-16	

Table I-42. GBM PE Ensemble Sampling Confusion Matrix and Statistics

Confusion Matrix		
	Reference	
Prediction	Postive	Negative
Positive	2	88
Negative	30	2288
Test Statistics		
Statistic	Value	
Accuracy	0.951	
95% CI	(0.942 0.959)	
Balanced Accuracy	0.513	
Sensitivity	0.063	
Specificity	0.962	
Pos Pred Value	0.022	
Neg Pred Value	0.987	
Mcnemar's Test P-value	<2e-16	

A..2.4 Random Forest Models

Table I-43. RF PE No Sampling Confusion Matrix and Statistics

Confusion Matrix		
	Reference	
Prediction	Postive	Negative
Positive	0	0
Negative	32	2376
Test Statistics		
Statistic	Value	
Accuracy	0.987	
95% CI	(0.981 0.991)	
Balanced Accuracy	0.500	
Sensitivity	0.000	
Specificity	1.000	
Pos Pred Value	NaN	
Neg Pred Value	0.986	
Mcnemar's Test P-value	4.25e-08	

Table I-44. RF PE Up Sampling Confusion Matrix and Statistics

Confusion Matrix		
	Reference	
Prediction	Postive	Negative
Positive	6	205
Negative	26	2171
Test Statistics		
Statistic	Value	
Accuracy	0.9041	
95% CI	(0.892 0.916)	
Balanced Accuracy	0.551	
Sensitivity	0.188	
Specificity	0.914	
Pos Pred Value	0.028	
Neg Pred Value	0.988	
Mcnemar's Test P-value	<2e-16	

Table I-45. RF PE Down Sampling Confusion Matrix and Statistics

Confusion Matrix		
	Reference	
Prediction	Postive	Negative
Positive	11	474
Negative	21	1902
Test Statistics		
Statistic	Value	
Accuracy	0.794	
95% CI	(0.777 0.810)	
Balanced Accuracy	0.572	
Sensitivity	0.344	
Specificity	0.801	
Pos Pred Value	0.022	
Neg Pred Value	0.989	
Mcnemar's Test P-value	<2e-16	

Table I-46. RF PE ROSE Sampling Confusion Matrix and Statistics

Confusion Matrix		
	Reference	
Prediction	Postive	Negative
Positive	32	2376
Negative	0	0
Test Statistics		
Statistic	Value	
Accuracy	0.013	
95% CI	(0.009 0.018)	
Balanced Accuracy	0.500	
Sensitivity	1.000	
Specificity	0.000	
Pos Pred Value	0.013	
Neg Pred Value	NaN	
Mcnemar's Test P-value	<2e-16	

Table I-47. RF PE SMOTe Sampling Confusion Matrix and Statistics

Confusion Matrix		
	Reference	
Prediction	Postive	Negative
Positive	0	1
Negative	32	2375
Test Statistics		
Statistic	Value	
Accuracy	0.986	
95% CI	(0.981 0.990)	
Balanced Accuracy	0.499	
Sensitivity	0.000	
Specificity	0.999	
Pos Pred Value	0.000	
Neg Pred Value	0.987	
Mcnemar's Test P-value	<2e-16	

Table I-48. RF PE Ensemble Sampling Confusion Matrix and Statistics

Confusion Matrix		
	Reference	
Prediction	Postive	Negative
Positive	0	0
Negative	32	2376
Test Statistics		
Statistic	Value	
Accuracy	0.987	
95% CI	(0.981 0.990)	
Balanced Accuracy	0.500	
Sensitivity	0.000	
Specificity	1.000	
Pos Pred Value	NaN	
Neg Pred Value	0.987	
Mcnemar's Test P-value	<2e-16	

Appendix II

Figures

A. Venous Thromboembolism Risk Prediction

A..1 Deep Venous Thrombosis

A..1.1 Training

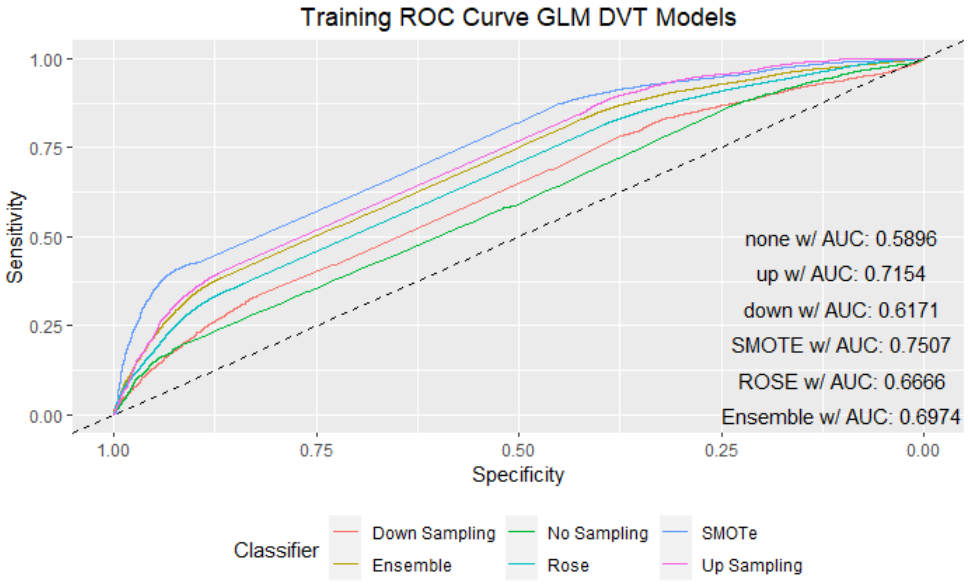

Figure II-1. GLM Training DVT ROC Curve

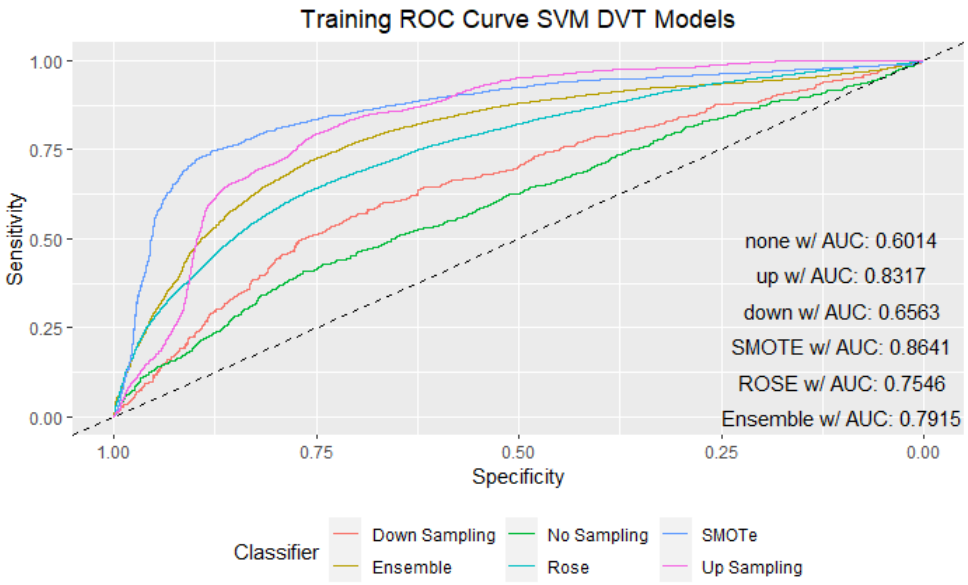

Figure II-2. SVM Training DVT ROC Curve

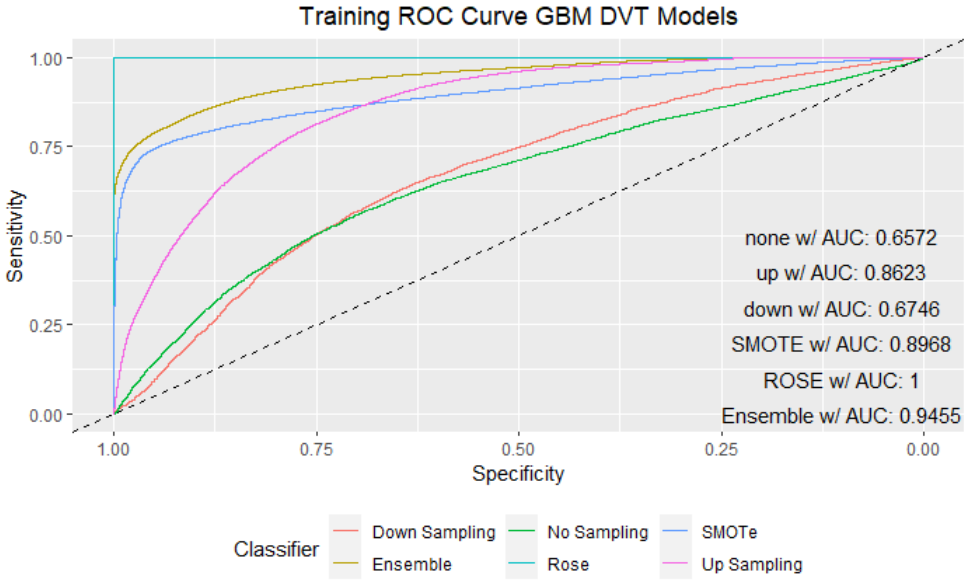

Figure II-3. GBM Training DVT ROC Curve

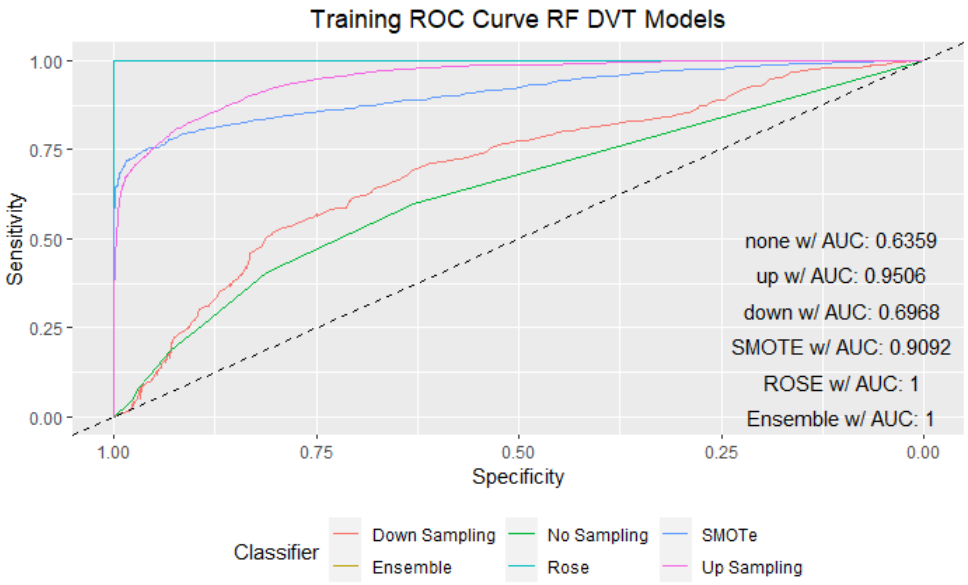

Figure II-4. RF Training DVT ROC Curve

A..1.2 Testing

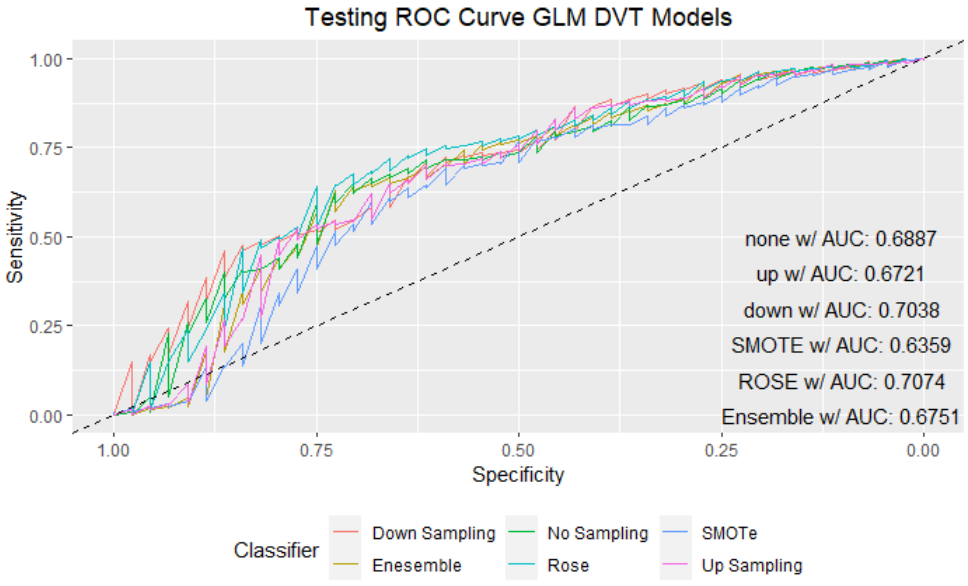

Figure II-5. GLM Testing DVT ROC Curve

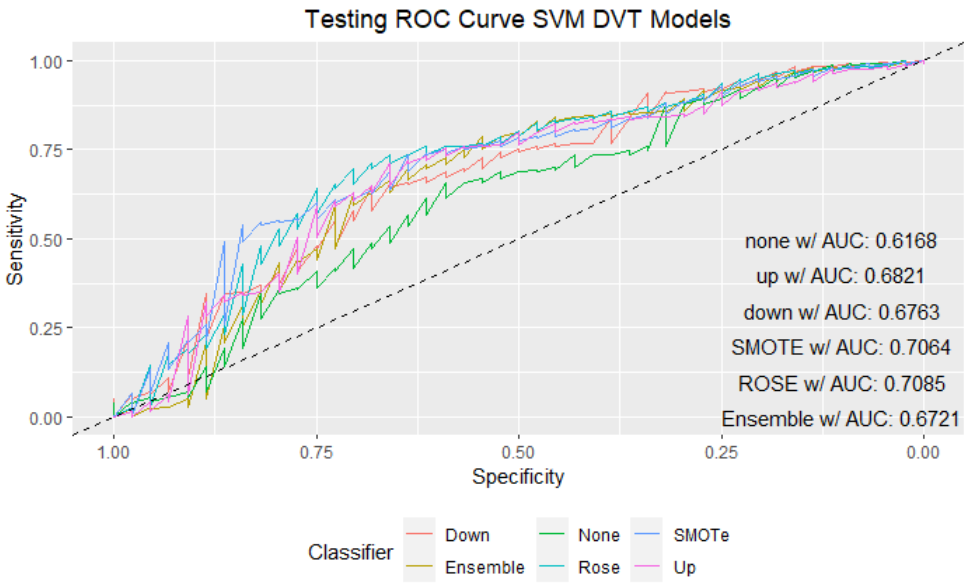

Figure II-6. SVM Testing DVT ROC Curve

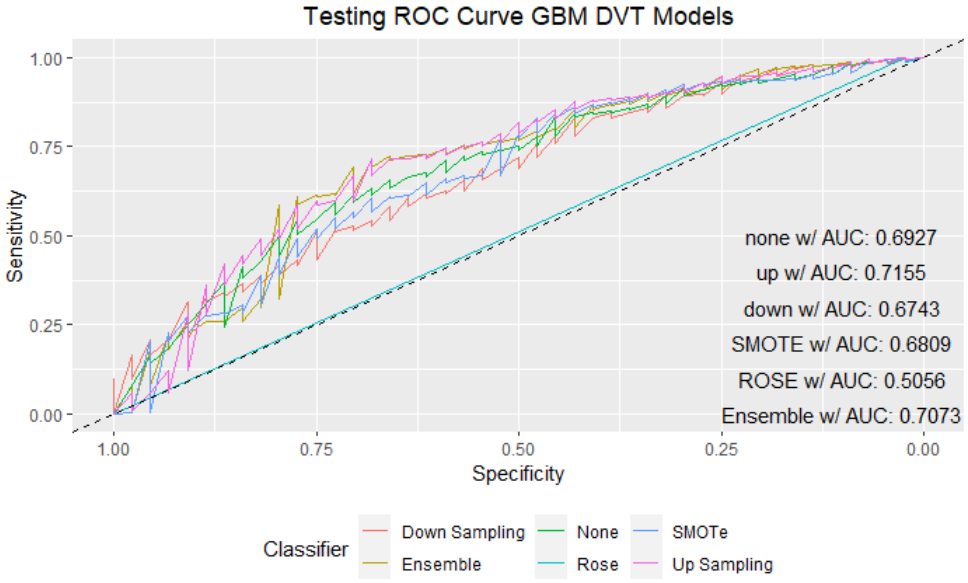

Figure II-7. GBM Testing DVT ROC Curve

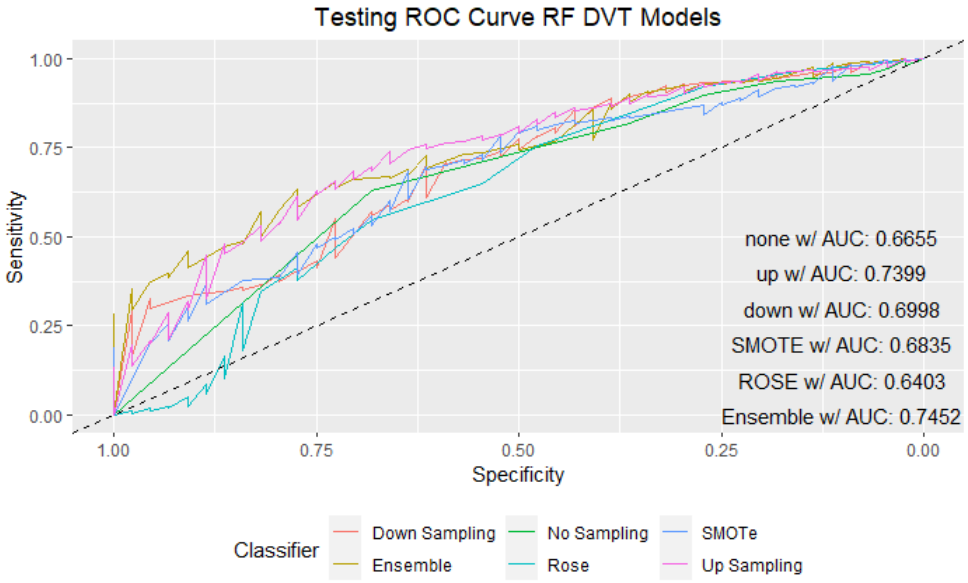

Figure II-8. RF Testing DVT ROC Curve

A..1.3 Feature Importance

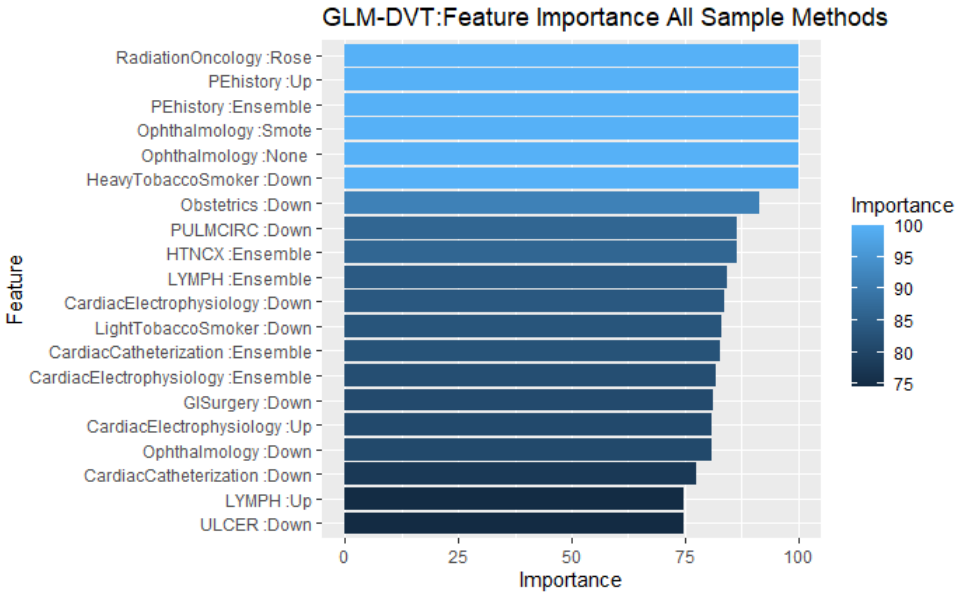

Figure II-9. GLM DVT Risk Prediction Feature Importance

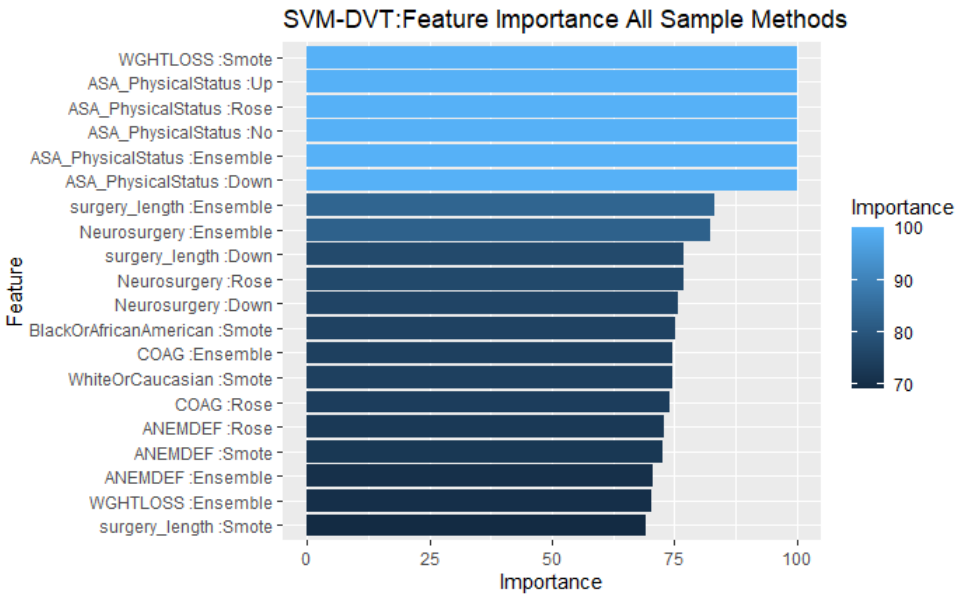

Figure II-10. SVM DVT Risk Prediction Feature Importance

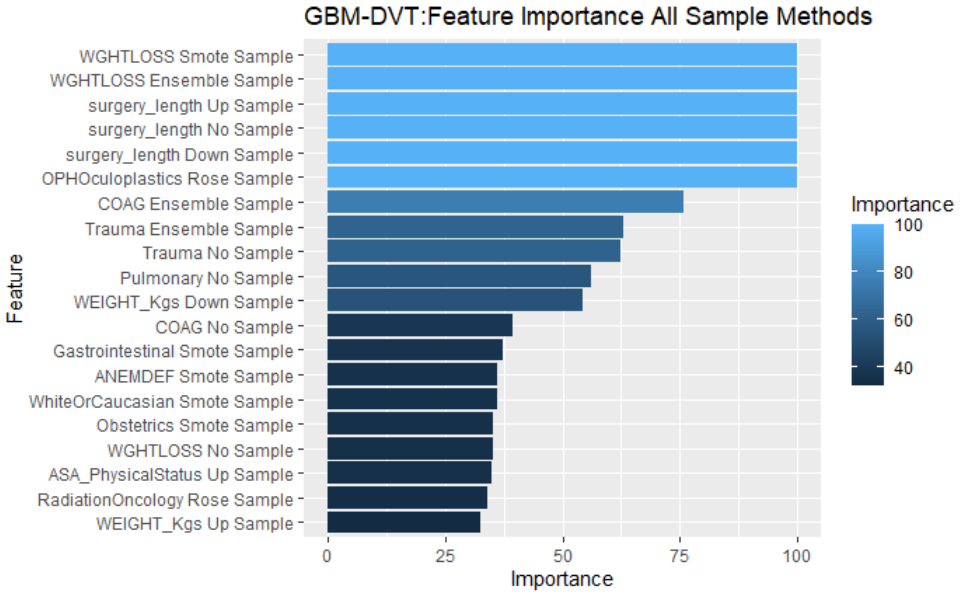

Figure II-11. GBM DVT Risk Prediction Feature Importance

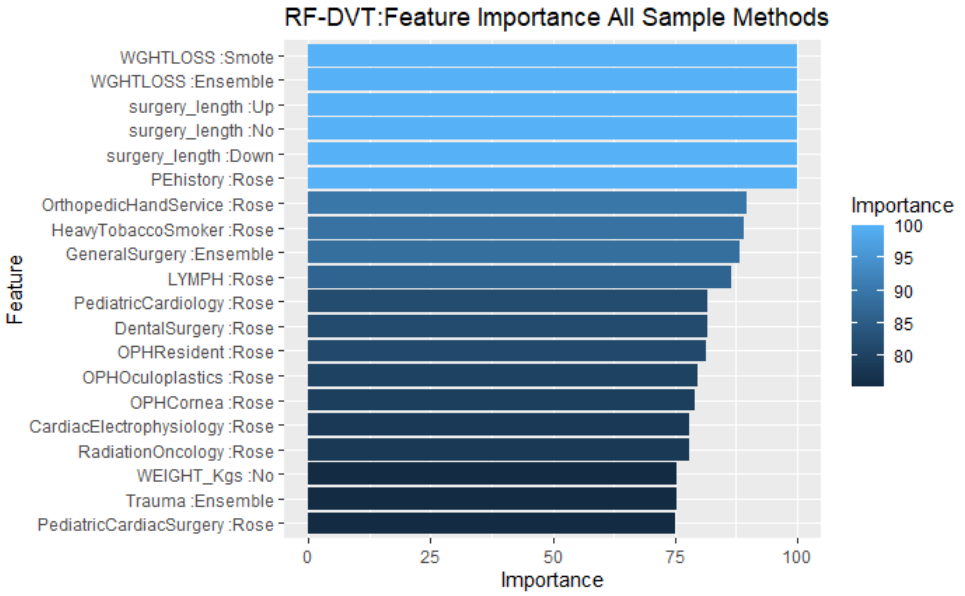

Figure II-12. RF DVT Risk Prediction Feature Importance

A..2 Pulmonary Embolisms

A..2.1 Training ROC Curves

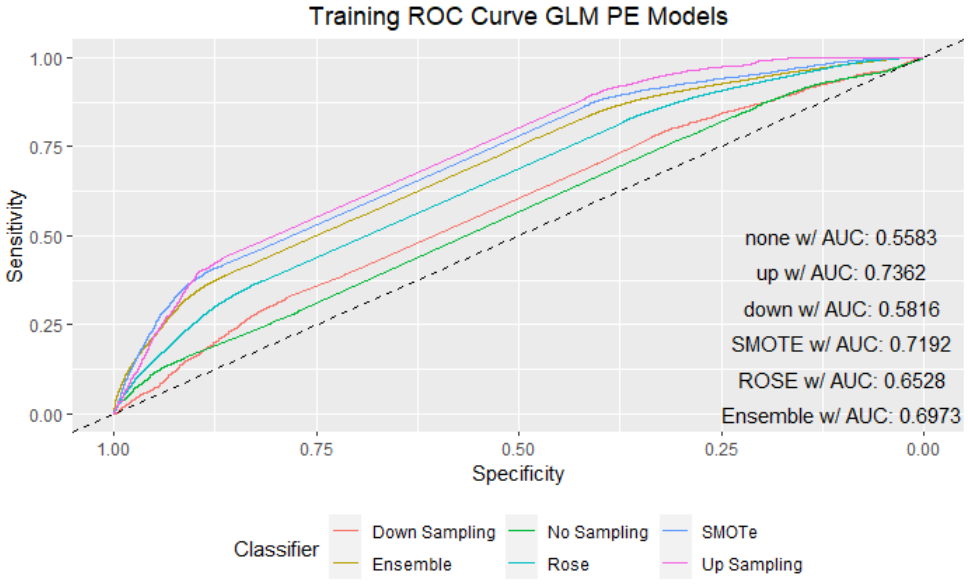

Figure II-13. GLM Training PE ROC Curve

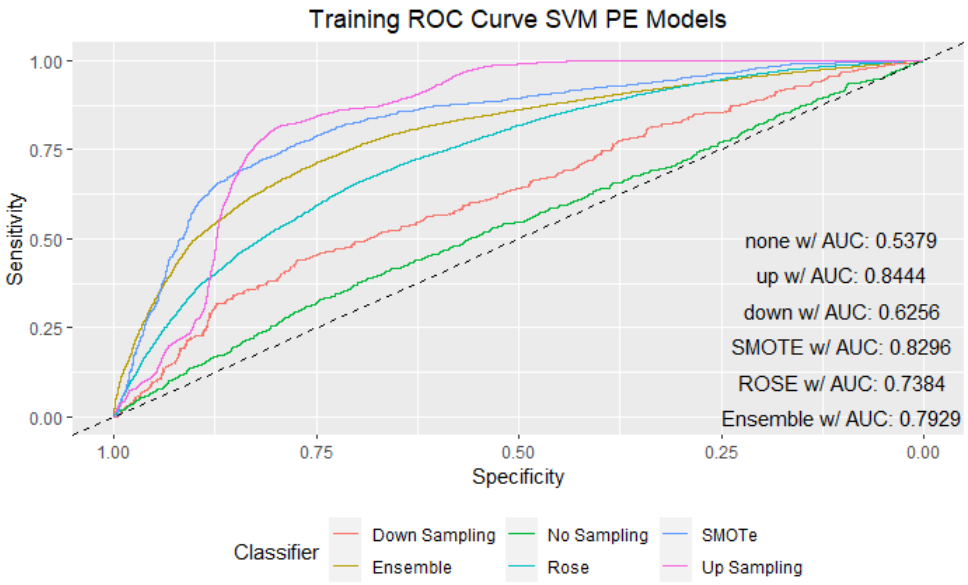

Figure II-14. SVM Training PE ROC Curve

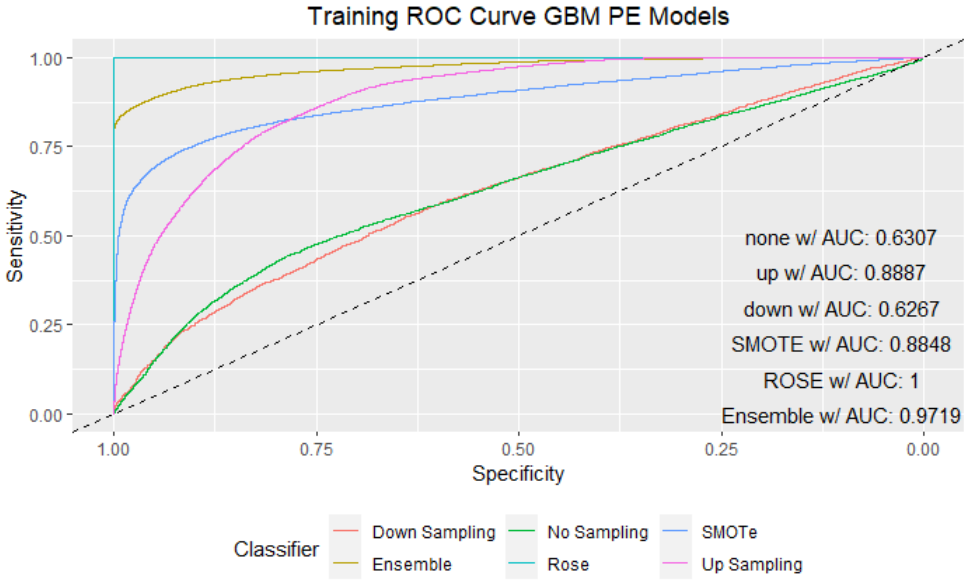

Figure II-15. GBM Training PE ROC Curve

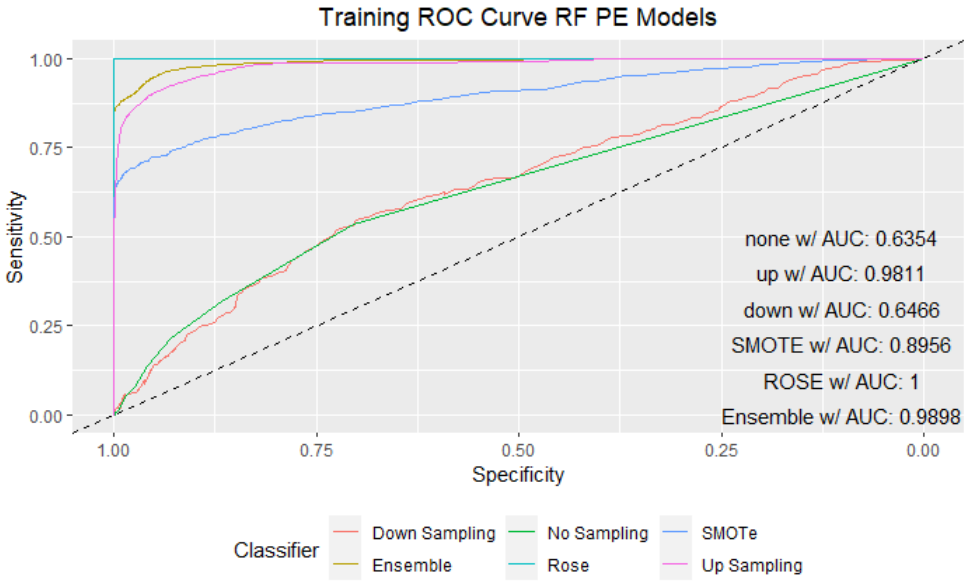

Figure II-16. RF Training PE ROC Curve

A..2.2 Testing ROC Curves

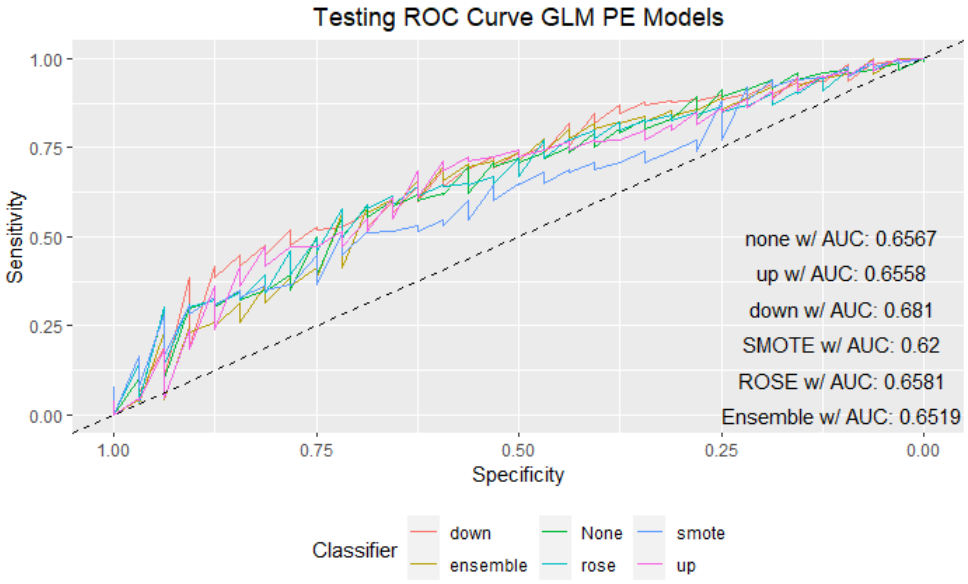

Figure II-17. GLM Testing PE ROC Curve

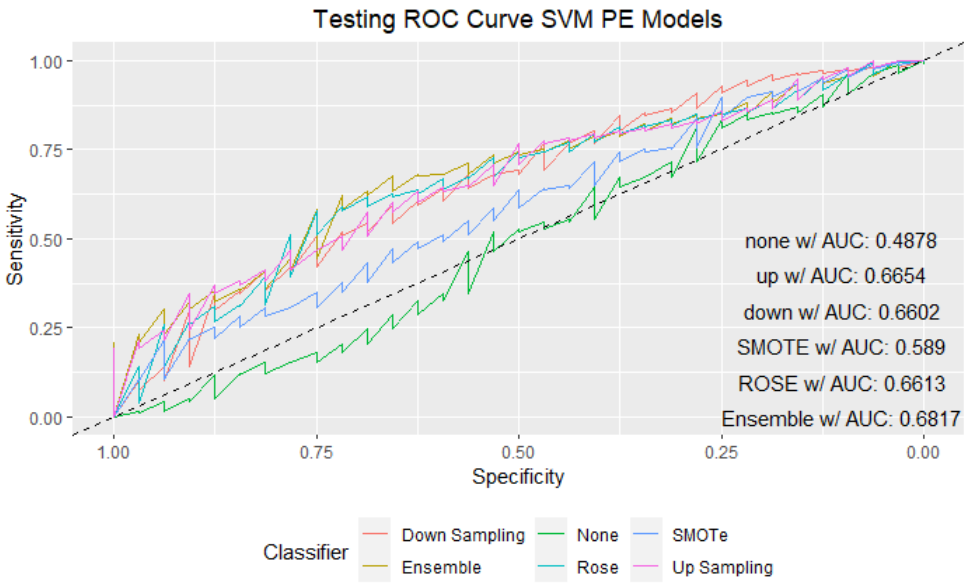

Figure II-18. SVM Testing PE ROC Curve

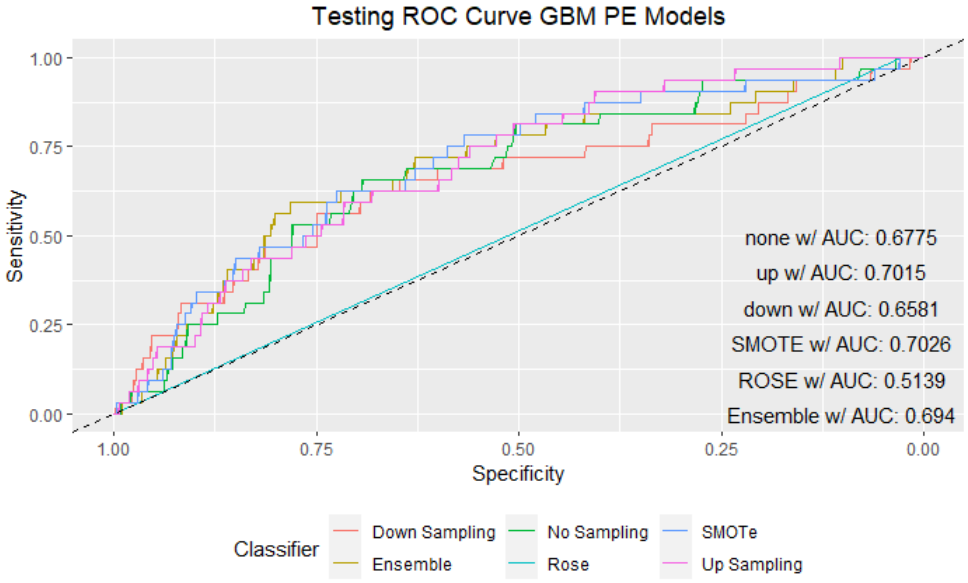

Figure II-19. GBM Testing PE ROC Curve

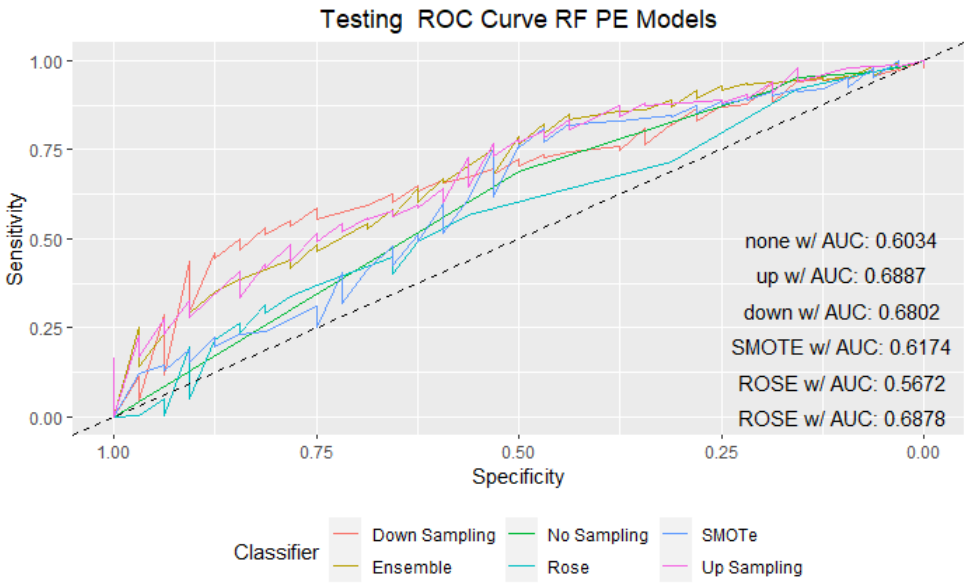

Figure II-20. RF Testing PE ROC Curve

A..2.3 Feature Importance

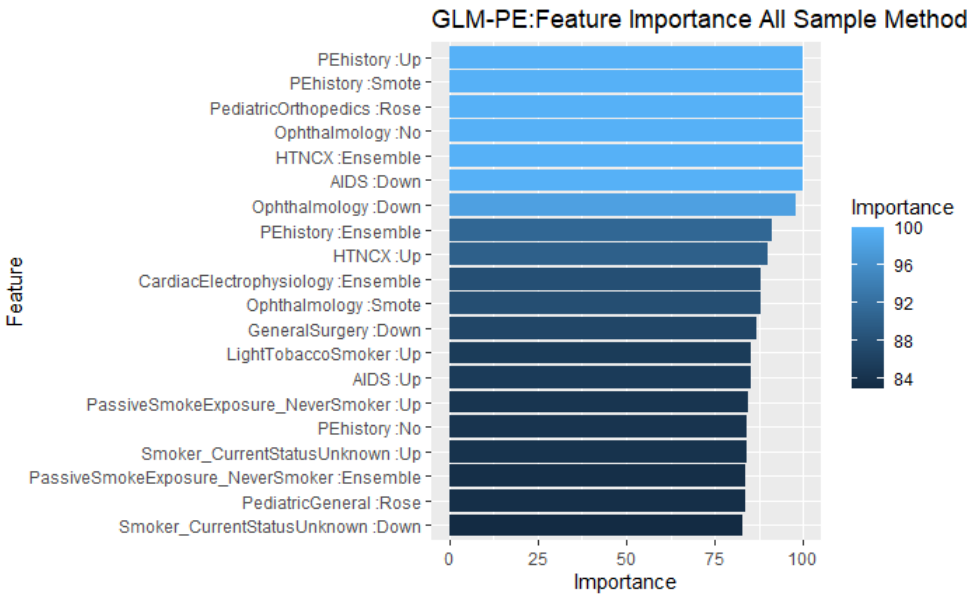

Figure II-21. GLM PE Risk Prediction Feature Importance

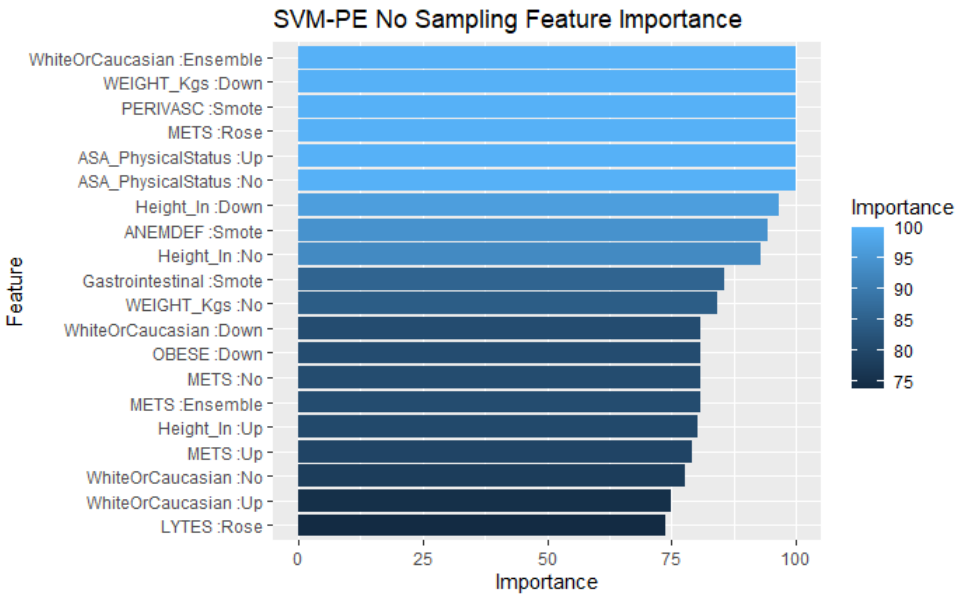

Figure II-22. SVM PE Risk Prediction Feature Importance

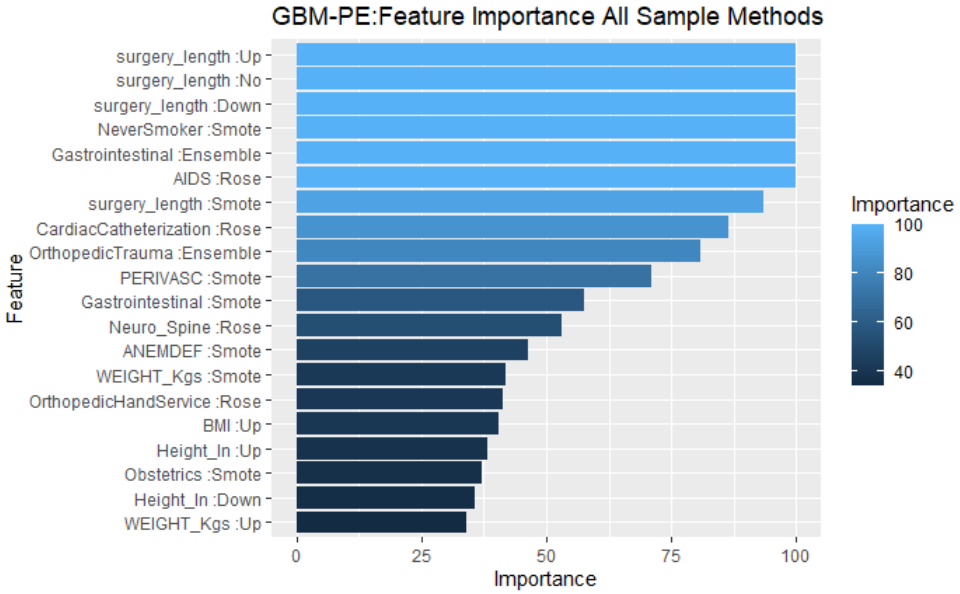

Figure II-23. GBM PE Risk Prediction Feature Importance

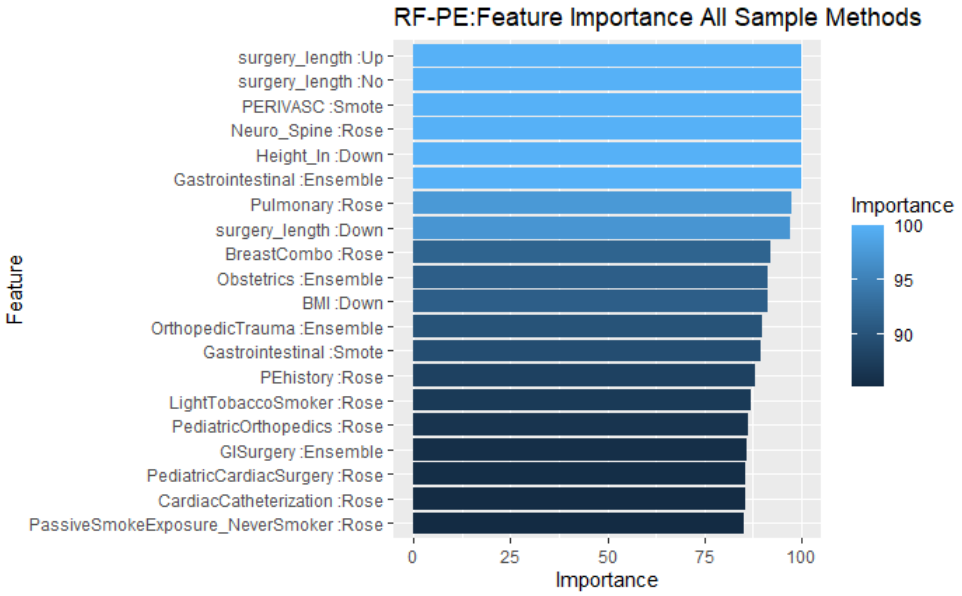

Figure II-24. RF PE Risk Prediction Feature Importance

B. Real Time VTE Risk Classification

B..1 VTE

B..1.1 ROC Curves

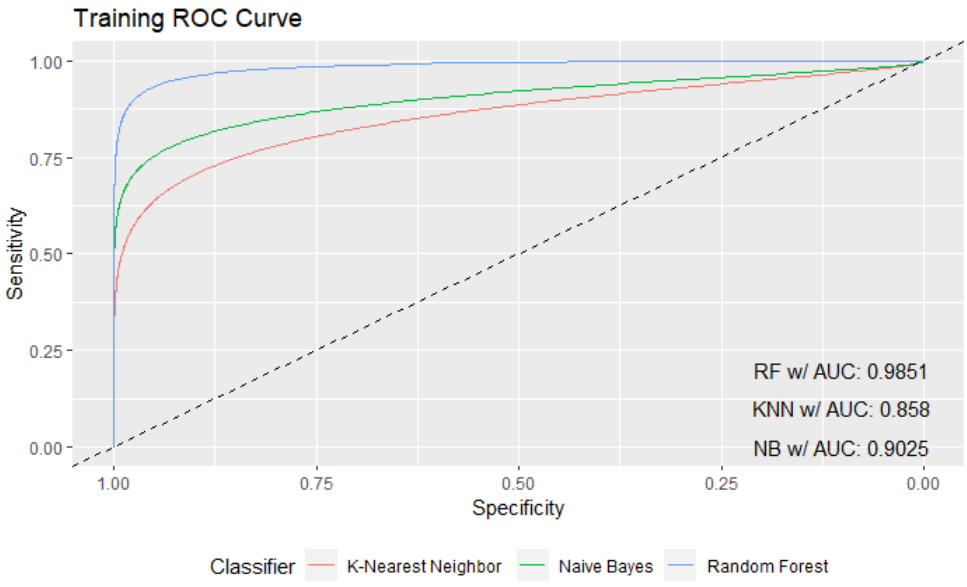

Figure II-25. Real Time VTE Training ROC Curves

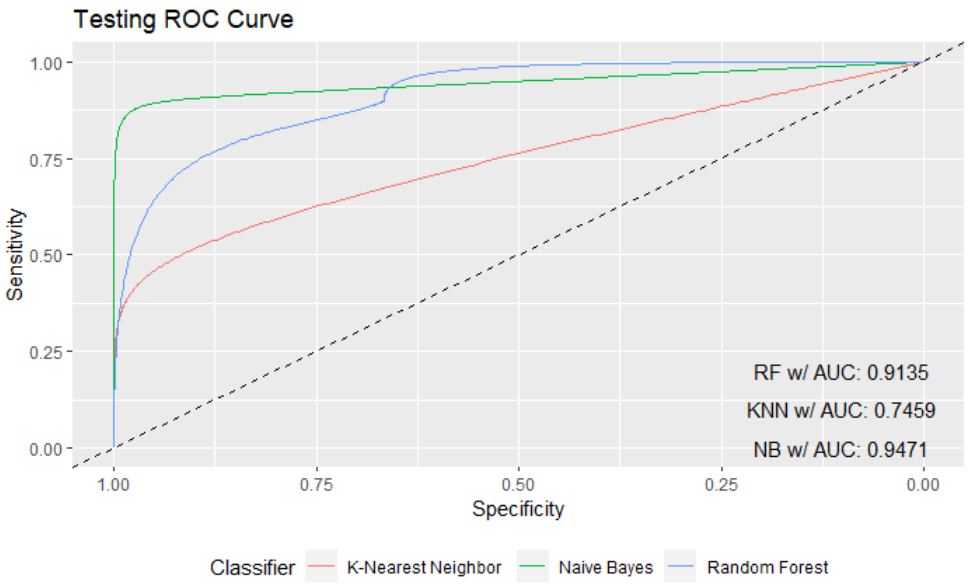

Figure II-26. Real Time VTE Testing ROC Curves

B..1.2 Feature Importance

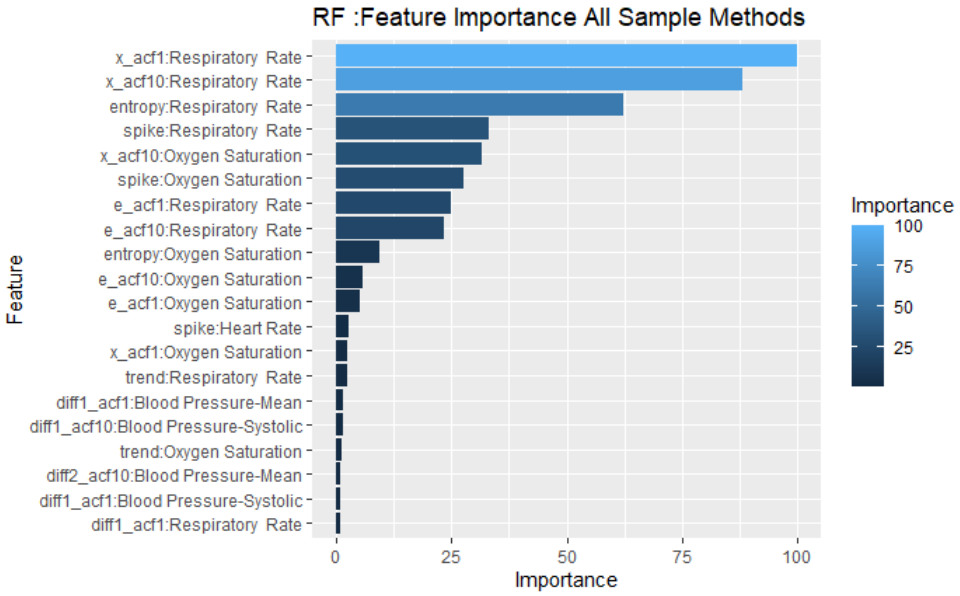

Figure II-27. RF VTE Real Time VTE Risk Classification Feature Importance

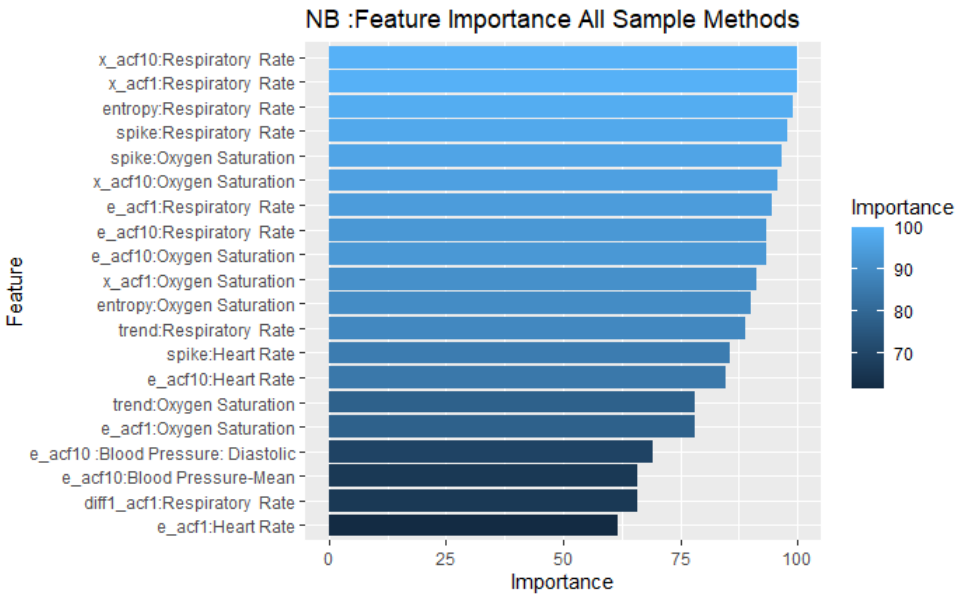

Figure II-28. NB VTE Real Time VTE Risk Classification Feature Importance

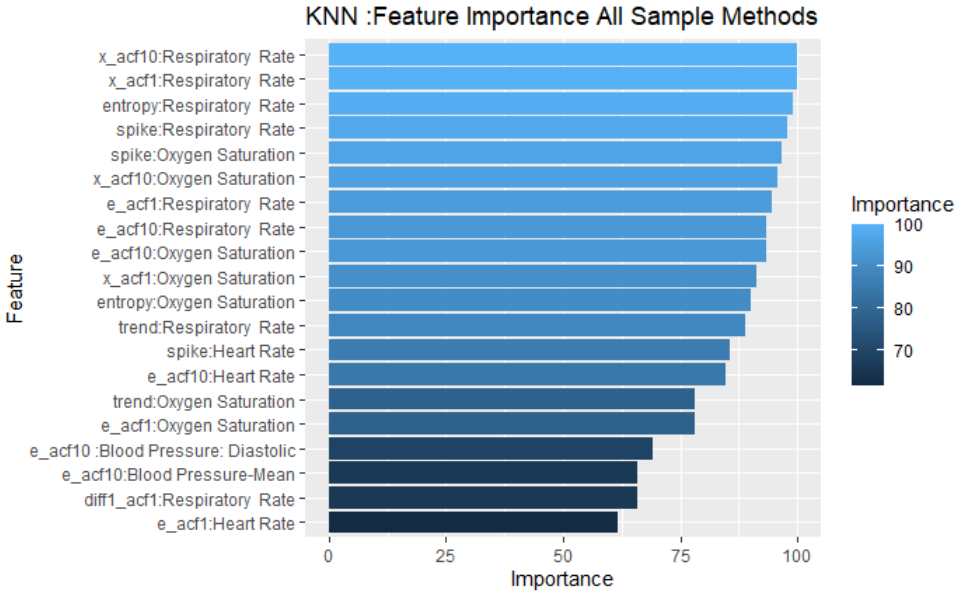

Figure II-29. KNN VTE Real Time VTE Risk Classification Feature Importance

AKILAN
MEIYAPPAN

3220 Cornell Lane, Ellicott City MD 21042
(410)-868-9263
m.akilan@gmail.com
www.linkedin.com/in/
akilan-meiyappan-aab886126

CAREER OBJECTIVE

To develop and establish expertise in the application of biomedical computing, with a strong focus on Data Science and Artificial Intelligence, to solve problems that can bring significant advancements in patientcare to meet the demands of precision-medicine and fulfill unsolved and unknown challenges.

EDUCATION

M.S.E Biomedical Engineering | Johns Hopkins University
AUGUST 2019 – CURRENT *(MAY 2021)*

Focus Area: Data Science

Thesis: Advanced Risk Stratification and Prediction of Venous Thromboembolism in Critically Ill Patients *(in preparation)*

B.S. Mechanical Engineering | University of Maryland, Baltimore County
AUGUST 2014 – DECEMBER 2018

MARRIOTT'S RIDGE HIGH SCHOOL |MARRIOTTSVILLE, HOWARD COUNTY MD
AUGUST 2010 – MAY 2014

EXPERIENCE

Research Intern | Johns Hopkins University
SEPTEMBER 2019 – CURRENT |DR. ADAM SAPIRSTEIN
Developed a Real-Time Risk Assessment Model to determine the likelihood of a Surgical ICU patient developing a Venous Thromboembolism (VTE) while in recovery. The model incorporates machine learning algorithms that analyzes high-frequency physiological time series data to determine the likelihood of a VTE.

Lab Assistant | SigTinc. Inc
JUNE 2019 – CURRENT |MR. PARAG KARMAKAR
Developed a Machine Learning algorithm for a new catheter system designed by Mr. Karmakar. This new system embeds tiny laser-sketched sensors to the three sides of the catheter tip, in order to sense what the catheter tip is in contact with. By labeling and analyzing key frequency points, the algorithm can predict what the contact tissue is without clinician input. Furthermore, a UI interface was developed for so clinicians can easily interpret predictions in a OR environment.

Teaching Assistant | University of Maryland, Baltimore County
OCTOBER 2018 – DECEMBER 2018 |DR. FIROOZ BAKHTIARI NEJAD
My duties as a Teaching Assistant are to incorporate fortifying exercises exhibited by educators by evaluating material with students one-on-one or in small groups, upholding school and class standards to help show students legitimate conduct, assisting instructors with record-keeping, for example, following participation and ascertaining evaluations, and helping educators get ready for exercises by preparing materials or setting up hardware, for example, PCs.

Lab Assistant | Johns Hopkins University
JUNE 2017 – AUGUST 2018 |DR. ISHAN BARMAN
Application of Deep/Machine Learning on different abnormal cells. Throughout my internship that spanned over two summers, two applications of deep learning were designed and developed. One was for image classification based on cell-lines and another on developing a neural network to enhance the resolution of an image (super-resolution)

Data Analyst | Johns Hopkins Medical Institutions
JUNE 2016 – AUGUST 2016 | DR. MICHAEL JACOBS
The project was a development of a Natural Language Processing tool based on IBM's UIMA framework for Unstructured Information Management Applications, to automatically identify and analyze keywords and phrases from Clinical Reports of Breast Cancer patients, to extract radiological parameters from the textual descriptions of the tumor, thereby enabling the classification of patient population to be able to better understand underlying relationship between the parameters that can help us advance our understanding of cancer treatment response - a major hurdle in breast cancer treatment.

Data Analyst | Johns Hopkins Medical Institutions
JUNE 2015 – AUGUST 2015 | DR. MICHAEL JACOBS
Developed a software program in Java that runs as a plug-in under ImageJ (a Medical Image Analysis program from National Institutes of Health) to process MRI datasets to create maps of Apparent Diffusion factor or Coefficient of water molecules in the tissue by curve fitting mono or bi-exponential equations through every individual pixel in the input datasets. Apparent Diffusion Coefficients (ADC) are considered as an extremely important parameter to characterize cancer tissues.

Summer Intern | Johns Hopkins Medical Institutions
JUNE 2014 – AUGUST 2014 | DR. ZAVER BHUJWALLA
Development of 3D animation using 3DsMax Software to effectively illustrate and visualize models of cancer development in humans using graphical animations of cell growth, invasion and metastasis in a human body.

Summer Intern | Johns Hopkins Medical Institutions
AUGUST 2013 – MAY 2014 | DR. STEVE CHO
Development of 3D interaction using Sony Play Station Move Controller for intuitive manipulation of medical images in 3D. Programming was based on Sony's Move.me interface software to recognize move controller's 3D motions and translate those motions to suitable mouse movement to manipulate the images displayed.

PUBLICATIONS

1. Karandikar, Sukrut ; Zhang, Chi; **Meiyappan, Akilan** ; Barman, Ishan; Finck, Christine; Srivastava, Pramod ; Pandey, Rishikesh, **Reagent-free and high-throughout assessment of T cell activation state using diffraction phase microscopy and deep learning,** *Analytical Chemistry, Feburary 2019*

2. [**Abstract**] Jinrui Liu, Ryan Brody, **Akilan Meiyappan**, Bronte Wen, Elizabeth Wu,Hieu Trung Nguyen, Hanbiehn Kim, Raimond Winslow, Joseph Greenstein, Adam Sapirstein, Sachidanand Hebbar, Nauder Faraday. **Advanced Risk Stratification and Prediction of Venous Thromboembolism in Critically Ill Patients**, *JHU Design Day, AI in Healthcare, November 2019*

PUBLIC HEALTH PROJECTS

COVID Mapping Project | Data Science for Public Health
SPRING 2020 | JOHNS HOPKINS UNVIERSITY
Developed a US Coronavirus Dashboard Map, which detailed basic public information such as number of positive, negative and hospitalized cases on a state-by-state basis. Information was curated and distributed via dashboard using R and Shiny.

Type 2 Diabetes Genomic Sequencing | Computational Biology & Bioinformatics
SPRING 2020 | JOHNS HOPKINS UNVIERSITY
Developed a machine learning model to predict whether or not an individual has Type 2 Diabetes based on their sequenced genomic data. All genomic data was obtained via open-source platforms such as openSNP and model was developed in R.

COURSEWORK PROJECTS

Global Nano-Brewery System Cooling | Mechanical Engineering System Designs
FALL 2018 | UNIVERSITY OF MARYLAND, BALTIMORE COUNTY
Designed a cooling system for a private nano-brewery system. The system had to properly heat and cool brew to a certain temperature in a given time as specified in the brew recipe. Furthermore, design had to take into consideration they physical limitations of the bar and kitchen where system would be placed.

Swiveling Basketball Mannequin | Engineering Design and Development
SENIOR YEAR| MARRIOTTS RIDGE HIGH SCHOOL
Designed and developed a swiveling basketball mannequin that mimics the real-life motion of a player defending an opposing player, to be used by players to individual practice. Swiveling motion was achieved thru the use of servo motor at the base which would swivel the mannequin.

PROGRAMING SKILLS

Scientific-Computing Programing Languages

- TensorFlow, Python
- R and Shiny (for Web Interface)
- MATLAB

General Purpose Programming Languages

- Java

OS / Database / Repository- Familiarity

- UNIX • WINDOWS • MacOS
- SQL
- Git-hub

Engineering Application Software

- Solid-Works
- 3DS Max

SOCIAL SKILLS

Executive Board Member | UMBC Minority Association for Pre-Medial Society

MAY 2017 – MAY 2018 | UNIVERSITY OF MARYLAND, BALTIMORE COUNTY

Planned and assisted for the execution of various fundraising activates and events aimed at informing students of proper study techniques and methods for education.

Executive Board Member | UMBC Bengali Student Council

MAY 2016 – MAY 2018 | UNIVERSITY OF MARYLAND, BALTIMORE COUNTY

Planned and organized events aimed to informing outside students about the cultures and traditions of Bangladesh. Served as Secretary and then Treasurer.

Volunteer | Tamil Entrepreneurs Forum (TEFCON) Conference

SUMMER 2016 | TRENTON, NJ

TEFCON is conference for Entrepreneurs, Business Executives, Venture Capitalists, Industry Influencers and Thought-Leaders from around the world with a shared common origin of Tamil language and culture. Volunteered to assist the presenters and attending guests when they needed help with technical issues.

Youth Volunteer | Tamil Sangam of Greater Washington

SUMMER 2010 – SUMMER 2014 | WASHINGTON, D.C.

Assisted with sorting out advisory group for overseeing children during the cultural event and aided the gathering of coordinators for stage arrangements for the cultural presentations. Volunteered to assist in the sale of traditional Indian food and snacks at the cultural event.

Biographical sketch

As a Biomedical Engineering Student with a focus area in Data Science, I have the experience and knowledge to carry the necessary tasks and requirements for the proposed research project. Throughout my graduate studies, I have worked on various Machine Learning and AI projects focused on improving healthcare needs of patients as well making it easier for physicians to properly diagnose and treat patients. In these projects I develop classification models to be used by clinicians in order to provide clinicians additional information, such as the probability of a patient developing a fatal disease during their admission in the hospital. Other projects include analyzing radio signals from catheters to determine type of contact tissue as well as using image classification models to classify Reagent T-cell images. My experience with machine learning gives me the ability to address complex challenges. Artificial Intelligence is a rapidly growing field and has shown to be vital in the health care setting to address the needs healthcare workers face on the front line. As such, my expertise with Machine Learning and Artificial Intelligence makes me a prime candidate in order to tackle the problems and challenges in the following project.